AD-A107 771 OKLAHOMA STATE UNIV STILLWATER DEPT OF PHYSICS F/G 20/6
STUDY OF DEFECTS PRODUCED BY THE GROWTH, POST TREATMENT AND FAB--ETC(U)
OCT 81 L E HALLIBURTON, J J MARTIN F19628-80-C-0086
RADC-TR-81-276 NL

UNCLASSIFIED

1 of 1
AD A107 771

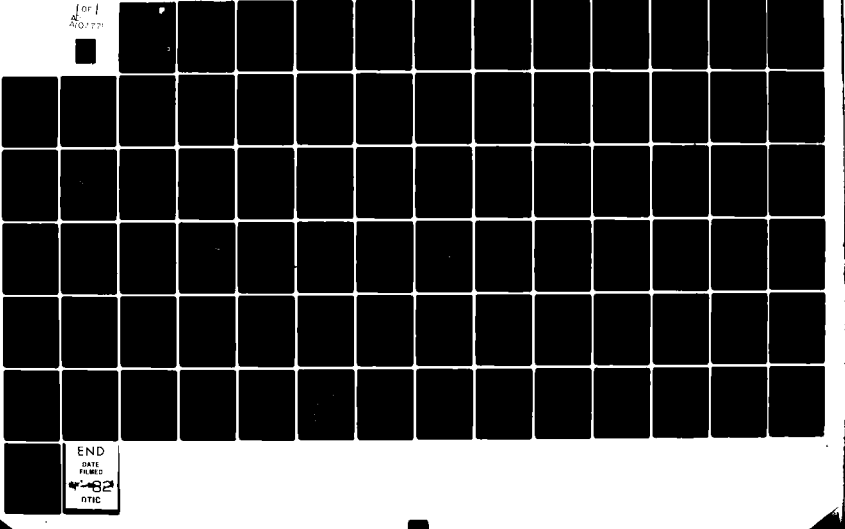

END
DATE FILMED
1-82
DTIC

LEVEL II (12)

RADC-TR-81-276
Interim Report
October 1981

STUDY OF DEFECTS PRODUCED BY THE GROWTH, POST TREATMENT AND FABRICATION OF QUARTZ

Oklahoma State University

Larry E. Halliburton
Joel J. Martin
William A. Sibley

ROME AIR DEVELOPMENT CENTER
Air Force Systems Command
Griffiss Air Force Base, New York 13441

This report has been reviewed by the RADC Public Affairs Office (PA) and is releasable to the National Technical Information Service (NTIS). At NTIS it will be releasable to the general public, including foreign nations.

RADC-TR-81-276 has been reviewed and is approved for publication.

APPROVED:

JOHN K. KENNEDY, Chief
Electromagnetic Materials Technology Branch
Solid State Sciences Division

APPROVED:

FREEMAN D. SHEPHERD
Acting Director
Solid State Sciences Division

FOR THE COMMANDER:

JOHN P. HUSS
Acting Chief, Plans Office

If your address has changed or if you wish to be removed from the RADC mailing list, or if the addressee is no longer employed by your organization, please notify RADC (ESM) Hanscom AFB MA 01731. This will assist us in maintaining a current mailing list.

Do not return copies of this report unless contractual obligations or notices on a specific document requires that it be returned.

UNCLASSIFIED

SECURITY CLASSIFICATION OF THIS PAGE (When Data Entered)

19 REPORT DOCUMENTATION PAGE	READ INSTRUCTIONS BEFORE COMPLETING FORM
1. REPORT NUMBER (18) RADC-TR-81-276	2. GOVT ACCESSION NO. AD-A100771 / 3. RECIPIENT'S CATALOG NUMBER 1
4. TITLE (and Subtitle) (6) STUDY OF DEFECTS PRODUCED BY THE GROWTH, POST TREATMENT AND FABRICATION OF QUARTZ	5. TYPE OF REPORT & PERIOD COVERED Interim Report, 15 Apr 80 — 15 Apr 81
	6. PERFORMING ORG. REPORT NUMBER N/A
7. AUTHOR(s) (10) Larry E. Halliburton, Joel J. Martin, William A. Sibley (15)	8. CONTRACT OR GRANT NUMBER(s) F19628-80-C-0086
9. PERFORMING ORGANIZATION NAME AND ADDRESS Oklahoma State University, Physics Department, Stillwater OK 74074 (16)	10. PROGRAM ELEMENT, PROJECT, TASK AREA & WORK UNIT NUMBERS 61102F (17) 2306J135 J1
11. CONTROLLING OFFICE NAME AND ADDRESS Deputy for Electronic Technology (RADC/ESM) Hanscom AFB MA 01731 (11)	12. REPORT DATE October 1981
	13. NUMBER OF PAGES 77
14. MONITORING AGENCY NAME & ADDRESS (if different from Controlling Office) Same (12) 82	15. SECURITY CLASS. (of this report) UNCLASSIFIED
	15a. DECLASSIFICATION/DOWNGRADING SCHEDULE N/A

16. DISTRIBUTION STATEMENT (of this Report)

Approved for public release; distribution unlimited.

17. DISTRIBUTION STATEMENT (of the abstract entered in Block 20, if different from Report)

Same

18. SUPPLEMENTARY NOTES

RADC Project Engineer: Alton F. Armington (ESM)

19. KEY WORDS (Continue on reverse side if necessary and identify by block number)

Quartz crystals	Infrared absorption	Aluminum-hole center
Radiation damage	ESR	Electron Center
Q^{-1} Measurements	Electrolysis	E' Center
		Thermoluminescence

20. ABSTRACT (Continue on reverse side if necessary and identify by block number)

At Oklahoma State University, we are using a number of experimental techniques to investigate the various as-grown and radiation-induced defects in commercially available high-quality synthetic quartz. Interstitial ions such as H^+, Li^+, and Na^+ as well as radiation-induced holes trapped at oxygen ions act as charge compensator's located adjacent to the aluminum and this gives rise to Al-OH^-, Al-Li^+, Al-Na^+, and Al-hole centers. Absolute concentrations of these compensated aluminum centers have been determined as a function of

DD FORM 1 JAN 73 1473 EDITION OF 1 NOV 65 IS OBSOLETE

UNCLASSIFIED 400790

SECURITY CLASSIFICATION OF THIS PAGE (When Data Entered)

irradiation and annealing temperature for a variety of samples, both swept and unswept. The various treatments simply exchange one ype of compensator for another at the aluminum sites and, within experimental error, the sum of the aluminum centers remains constant for a given sample. This direct accountability of all the aluminum ions in hydrogen-swept samples strongly suggests that the 3306 and 3367 cm^{-1} infrared bands are associated with the Al-OH^- center. Also, the ESR and IR results show that the aluminum content of randomly selected bars of high-quality quartz can vary by an order of magnitude.

Acoustic loss measurements on a 5 MHz 5th overtone resonator blank show no loss peaks that can be attributed to the Al-Li^+ center, even though the blank was fabricated from a high-aluminum-content Premium Q bar and had been Li-swept, i.e., Li was swept into the blank. The Al-Na^+ center loss peak was removed by the Li sweep. Irradiation of unswept, Li-swept, and H_2-swept blanks at room temperature introduces loss peaks at 25 K, 100 K and 135 K. Since these three peaks anneal between 250 and 300°C, the same as the Al-hole center electron spin resonance spectrum, we conclude that the three peaks are caused by the Al-hole center. In unswept blanks, the Al-Na^+ loss peak is removed by radiation at room temperature but recovers upon annealing to temperatures above 350°C. The decay of the Al-OH^- center correlates with the recovery of the Al-Na^+ center in unswept material.

A series of oxygen-vacancy-associated centers have been discovered by ESR and are labeled E_1'', E_2'', and E_3'' centers. These are S = 1 centers and they appear to contain two adjacent oxygen vacancies. They are only found in unswept samples. i.e., samples containing interstitial alkali ions, although the interstitial alkali ion is not a component of the centers. Production and thermal decay characteristics are described in detail.

An investigation of the thermally stimulated luminescence, TSL, from quartz irradiated at 95K has been made below room temperature. It was determined that three regions of TSL glow peak interest exist. Region I (115-145 K) contains a single sharp peak having a maximum in its broad spectral emission at about 450 nm; Region II (145-185 K) is quite complex in structure, and is dependent upon defect content and sample treatment; Region III (185-270 K) can be eliminated by sweeping or by irradiation at temperatures above 250 K prior to the 95K irradiation. Both Regions II and III show broad band spectral emission with maxima near 380 nm. The intensity of the TSL glow peak in Region III appears to correlate well with the presence of Al-Na^+ and/or Al-Li^+ centers as determined from other measurements, suggesting it may provide yet another method for quartz crystal quality evaluation.

TABLE OF CONTENTS

I. INTRODUCTION AND SUMMARY

Alpha-quartz is used in a variety of electronic devices (e.g., high-precision oscillators, filters, accelerometers, etc.) where sensitivity and stability are crucial operating criteria. Since many of these applications require operation of the device in a radiation environment, considerable effort has been directed in recent years toward understanding the radiation response of quartz. It is now well-known that quartz-stabilized oscillators exposed to ionizing radiation (i.e., x-rays and gamma rays as well as high energy electrons, protons, and neutrons) may exhibit transient and steady-state changes in frequency and associated reductions in Q.[1-3] Early results obtained by King[4] and other investigators[5-8] suggested that these deleterious effects in the quartz oscillators were associated with the presence of impurities. This has led to increased study of the general behavior of impurities in quartz and there have been attempts to correlate observed frequency offsets with specific impurity-related radiation-induced defects.[9]

At Oklahoma State University, we have used a number of experimental techniques to investigate the various as-grown and radiation-induced defects in quartz. Electron spin resonance (ESR) and infrared absorption (IR) experiments have provided information about the role of aluminum in the radiation response of commercially available high-quality synthetic quartz. Samples obtained from two separate sources were investigated and identical radiation responses were found for the two materials. Interstitial ions such as H^+, Li^+, and Na^+ as well as radiation-induced holes trapped at oxygen ions act as charge compensators for the ever-present substitutional aluminum ions. Usually the charge compensator is located adjacent to the aluminum and this gives rise to $Al\text{-}OH^-$, $Al\text{-}Li^+$, $Al\text{-}Na^+$, and Al-hole centers. Absolute concentrations of these compensated aluminum centers have been determined as a function of irradiation and annealing temperature for a variety of samples, both swept and unswept. The various treatments

simply exchange one type of compensator for another at the aluminum sites and, within experimental error, the sum of the aluminum centers remains constant for a given sample. This direct accountability of all the aluminum ions in hydrogen-swept samples strongly suggests that the 3306 and 3367 cm^{-1} infrared bands are associated with the $Al\text{-}OH^-$ center. Also, the ESR and IR results show that the aluminum content of randomly selected bars of high-quality quartz can vary by an order of magnitude.

Acoustic loss measurements on a 5 MHz 5th overtone resonator blank show no loss peaks that can be attributed to the $Al\text{-}Li^+$ center, even though the blank was fabricated from a high-aluminum-content Premium Q bar and had been Li-swept, i.e., Li was swept into the blank. The $Al\text{-}Na^+$ center loss peak was removed by the Li sweep. Irradiation of unswept, Li-swept, and H_2-swept blanks at room temperature introduces loss peaks at 25 K, 100 K and 135 K. In H_2-swept material these peaks are approximately a factor of five smaller than the same peaks in similar unswept or Li-swept blanks. Since these three peaks anneal between 250 and 300°C, the same as the Al-hole center electron spin resonance spectrum, we conclude that the three peaks are caused by the Al-hole center. In unswept blanks, the $Al\text{-}Na^+$ loss peak is removed by radiation at room temperature but recovers upon annealing to temperatures above 350°C. The decay of the $Al\text{-}OH^-$ center correlates with the recovery of the $Al\text{-}Na^+$ center in unswept material.

An investigation of the thermally stimulated luminescence, TSL, from quartz irradiated at 95 K has been made below room temperature. The synthetic quartz specimens were of very high quality with a Q of about 10^6. Such material contains few impurities and the TSL is weak. Nonetheless, it was determined that three regions of TSL glow peak interest exist. Region I (115-145 K) contains a single sharp peak having a maximum in its broad spectral emission at about 450 nm; Region II (145-185 K) is quite complex in structure, and is dependent upon defect content and sample treatment; Region III (185-270 K) can be eliminated by electrodiffusion

("sweeping") techniques or by irradiation at temperatures above 250 K prior to the 95 K irradiation. Both Regions II and III show broad band spectral emission with maxima near 380 nm. The intensity of the TSL glow peak in Region III appears to correlate well with the presence of $A\ell$-Na^+ and/or $A\ell$-Li^+ centers as determined from other measurements, suggesting it may provide yet another method for quartz crystal quality evaluation.

II. THE ROLE OF ALUMINUM IMPURITIES

A. Introduction

Aluminum is the most pervasive impurity in both natural and synthetic quartz. These aluminum ions exist in the 3+ valence state in quartz and easily substitute for silicon, thus requiring charge compensation (i.e., an aluminum ion needs an additional positive-charged entity in the lattice to compensate for the charge of the replaced silicon). Examples of such charge compensators in quartz are H^+, Li^+, or Na^+ ions at interstitial sites or holes trapped at oxygen ions. Because of the strong Coulombic attraction force of the interstitial ions and the holes with the aluminum and because of the high mobility of both the interstitial ions and the holes, these charge compensators are usually located adjacent to the substitutional aluminum ions and this gives rise to either $A\ell$-OH^-, $A\ell$-Li^+, $A\ell$-Na^+, or Al-hole centers. Schematic representations of these various compensated aluminum centers are contained in Fig. 1.

The defect centers produced by local compensation of the substitutional aluminum ions can be experimentally observed by widely varying techniques. In the case of the $A\ell$-OH^- center, the interstitial proton bonds to an oxygen ion to form an OH^- molecule adjacent to the aluminum and infrared absorption provides a direct monitor of the center. Formation of the Al-hole center by trapping a hole at an oxygen ion adjacent to the aluminum results in an unpaired electron, and thus a paramagnetic defect, which can easily be detected by electron spin resonance (ESR).

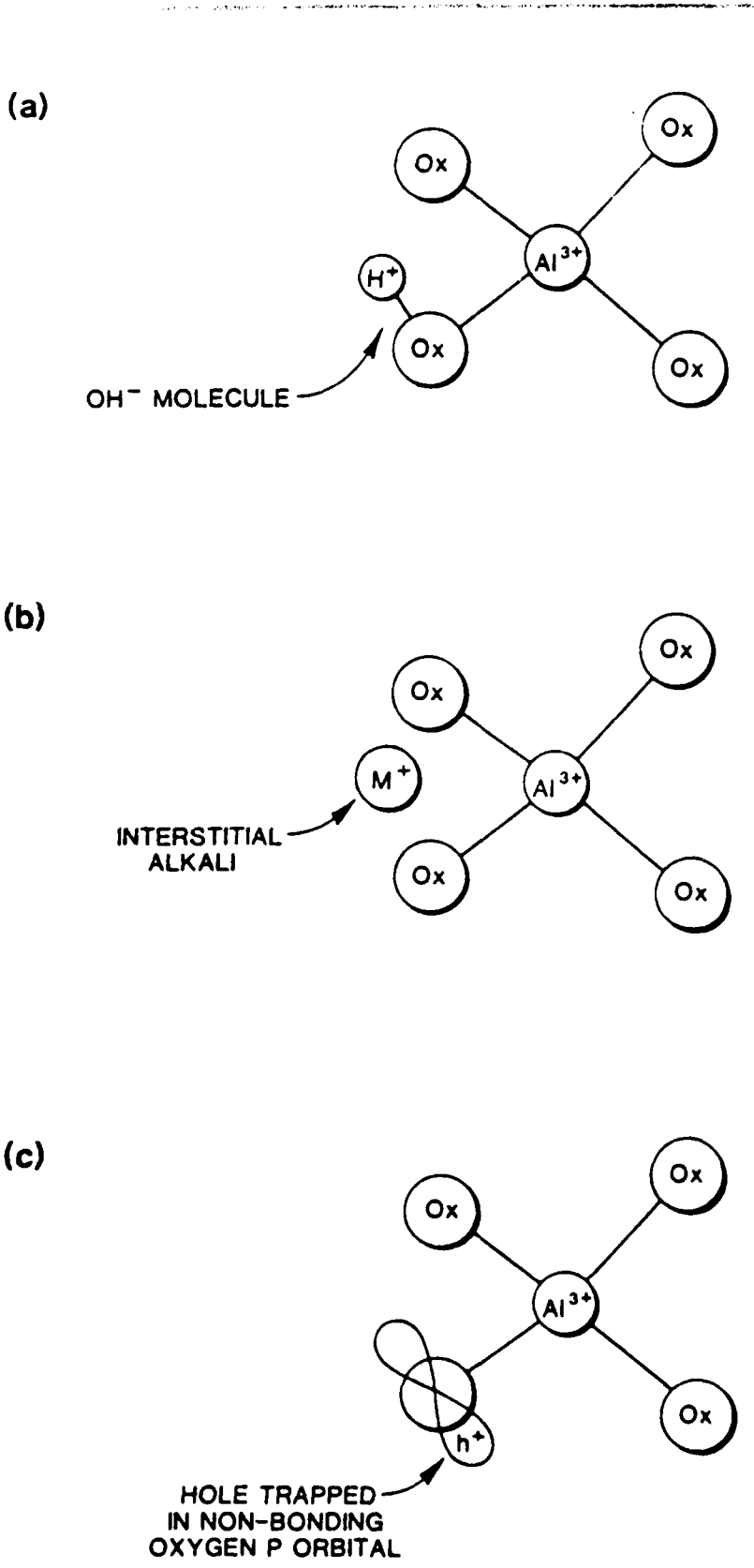

Figure 1. Schematic representation of (a) the Aℓ-OH^- center, (b) the Aℓ-M^+ center where M^+ is either Li^+ or Na^+, and (c) the $[Al_e+]^\circ$ center.

The Al-M^+ centers (where M^+ represents an alkali ion) exhibit no characteristic infarared bands and are not paramagnetic, but do cause a local lattice deformation. As a result, they can couple to external forces acting along certain crystallographic directions and can undergo a deformation relaxation with an attendant mechanical loss.

The electrodiffusion (sweeping) process initially developed by King[4] provides a method for changing the concentration of specific interstitial cations (i.e., H^+, Li^+, Na^+, etc.) within a given quartz crystal. This technique consists of applying an electric field parallel to the c-axis of the crystal while maintaining the sample temperature in the 400-550°C range. Either a vacuum or an inert gas, air, or hydrogen atmosphere surrounds the crystal. As positive-charged species are pulled along the large c-axis channels and out of the crystal by the electric field, additional positive-charged species of a similar or different nature are taken into the crystal at the opposite electrode in order to maintain charge neutrality for the sample as a whole. For example, if either air or a hydrogen atmosphere surrounds the crystal, the sweeping process will remove interstitial alkali ions from the crystal and replace them with H^+ ions. Numerous cases exist in the literature where the sweeping process has greatly helped in clarifying the behavior of various points defects in quartz.

In the present work, we have combined infrared and ESR data to obtain information about the formation and decay of the various aluminum centers in both swept and unswept high-quality synthetic quartz. By monitoring the absolute concentration of each type of compensated aluminum center (i.e., Al-OH^-, Al-M^+, or Al-hole after each step of a series of irradiations and anneals, we have shown, within experimental error, that the sum of these centers remains constant and that different treatments simply change one type of compensator for another. This direct accountability of all the aluminum ions within a crystal strongly suggests that the 3306 and 3367 cm^{-1} infrared bands are associated with the Al-OH^- center

and also reinforces the conviction that radiation-induced mobility of interstitial ions is the fundamental radiation response of quartz.

B. Background

1. Infrared Absorption

Quartz exhibits a large number of infrared absorption bands in the 3200 to 3600 cm^{-1} spectral region and Kats[10] has shown that many of these bands are due to OH^- stretching vibrations. However, it has proven extremely difficult to assign specific defect models to each of the OH^- absorption bands. Many researchers have focused attention on the two bands at 3306 and 3367 cm^{-1}. Normally, the 3367 cm^{-1} band is approximately three times more intense than the 3306 cm^{-1} band. Kats[10] observed these two bands in both natural and synthetic quartz and found that x-irradiation at room temperature enhanced their intensities. Also, Kats observed that sweeping in air strongly increased the two bands in synthetic samples and he tentatively suggested the two bands arise from an OH^- molecule adjacent to a substitutional aluminum.

Brown and Kahan[11] provided further evidence supporting the model proposed by Kats and also pointed out that failure to observe the 3306 and 3367 cm^{-1} bands did not necessarily mean a low aluminum content for the quartz crystal. They found that these two bands were not present initially in high-quality unswept quartz but were introduced by irradiation at room temperature. This, in turn, led Brown and Kahan to conclude that all of the substitutional aluminum ions are alkali-compensated in the as-grown high-quality quartz (i.e., before irradiation or sweeping).

Lipson et al.[12,13] have investigated the polarization of the 3306 and 3367 cm^{-1} bands and have demonstrated the strong temperature dependence of their half-widths (i.e., a narrowing at lower temperature). They found that heating to 500°C in a nitrogen atmosphere for long periods of time without application of an

electric field did not introduce the 3306 and 3367 cm^{-1} bnads in quartz. They also found that sweeping the quartz in a vacuum failed to introduce significant 3306 and 3367 cm^{-1} bands.

Recently, Sibley et al.[14] extended the study of the 3306 and 3367 cm^{-1} bands to include irradiations at various temperatures from 15 K to 300 K and to include thermal anneals from 77 K to 750 K. They found that although room temperature irradiation introduced these two bands in unswept synthetic quartz, a subsequent intense 77 K irradiation destroyed the two bands. Following the room temperature irradiation and subsequent 77 K irradiation, Sibley et al. found that the two bands slowly recovered with nearly equal intensities up to approximately 200 K, but in the 230-270 K anneal region the 3367 cm^{-1} band continued to grow while the 3306 cm^{-1} band decreased in intensity. At room temperature the bands had attained their usual intensity ratio. This sudden reversal of intensities in the 230-270 K region suggested the two bands arise from OH^- molecules in two different but closely related site symmetries and that a transfer from one site to the other (or a reorientation) occurs in the 230-270 K region.

2. Electron Spin Resonance

The Al-hole center is perhaps the best characterized of the point defects in quartz. The first observations of this center were by electron spin resonance and were reported by Griffiths, Owen, and Ward.[15] O'Brien[16] immediately offered an interpretation of the ESR data in terms of a model having a hole trapped primarily in a nonbonding orbital of an oxygen ion adjacent to a substitutional aluminum ion (see Fig. 1c). Mackey[17] greatly expanded this early work by discovering a family of $[Al_e+/M^+]^+$ centers when germanium-doped quartz was irradiated at 77 K. The M^+ represents an interstitial cation (i.e., either H^+, Li^+, or Na^+) which is trapped on one side of the aluminum ion while the hole remains trapped on the other side of the aluminum. These interstitial-compensated aluminum-hole centers have been further characterized by Mackey et al.[18] and by Nuttall.[19]

In α-quartz, the four oxygens surrounding a silicon (or aluminum) atom are only pairwise-equivalent, short- and long-bond oxygens. Kittal[19] has shown that the ground state of the Al-hole center corresponds to trapping the hole on a long-bond oxygen and Schnadt and Schneider[20] have shown that only 0.03 eV of energy is required to transfer the hole from one type of oxygen to the other. Precise values of the Al-hole center ground-state spin Hamiltonian hyperfine parameters have been obtained by Barker[21] using ENDOR techniques. Recently, Markes and Halliburton[22] have investigated the production and stabilization conditions for Al-hole centers and Koumvakalis[23] has correlated the Al-hole center ESR spectrum with a visible optical absorption. The comprehensive review by Weil[24] summarizes much additional work on the aluminum-associated hole centers in quartz.

C. Experimental

The α-quartz used in the present investigation was all pure Z-growth material and included Electronic Grade and Premium Q bars[25] obtained from Sawyer Research Products, Eastlake, Ohio and a Supreme Q bar obtained from Toyo Communications Equipment Company, Kawasaki, Japan. The sample labeling scheme introduced by Markes and Halliburton[22] has been followed in the present report. Impurity analysis along with autoclave and sweeping information for some of the Sawyer samples used in the present study are included in Reference 22. The Toyo bar SQ-A had been numbered 40-57 by the manufacturer. Infrared and ESR samples were taken from adjacent positions in each of the quartz bars and the same sample number was used for both components of a pair. For example, the sample number PQ-E10 actually represents both an infrared and an ESR sample in this paper. One of the pairs of samples cut from the Toyo bar was swept at Oklahoma State University (graphite electrodes, hydrogen atmosphere, 1600 volts/cm, 500°C, and 19 hrs duration). All sweeping of Electronic Grade and Premium Q bars was done by Sawyer in air.

The infrared samples were cut in the form of plates (15 x 15 x 3 mm^3)

perpendicular to the c-axis of the crystal. A Beckman 4240 spectrophotometer was used to measure the infrared absorption. During the measurements, samples were oriented such that the incident monitoring light was parallel to the c-axis (i.e., the electric vector of the unpolarized incident light was always perpendicular to the c-axis). All the infrared data were obtained near 77 K using a metal Dewar equipped with CaF_2 windows for the light beam. During irradiations, the tail of the Dewar was rotated 90°, thus positioning a 0.005 inch thick aluminum window in front of the sample.

The ESR spectrometer utilized a homodyne microwave bridge of our own design (operating near 9.1 GHz) and a 9-inch Fieldial-regulated Varian magnet. The magnetic field modulation frequency was 100 kHz. All the ESR data were taken at 77 K using a glass finger Dewar inserted in a Varian V-4531 rectangular cavity. The ESR samples were rectangular in shape (8 x 3 x 2 mm^3) and, during measurements, the magnetic field was always aligned parallel to the crystal c-axis.

Irradiations were 4 minutes in duration and used 1.7 MeV electrons from a Van de Graaff accelerator. The current on the sample was 0.2 $\mu A/cm^2$, corresponding to a dose of 3 x 10^7 rad(Si). During a 77 K irradiation, the ESR sample was immersed in liquid nitrogen, and then subsequently transferred into the glass finger Dewar. For an intermediate temperature irradiation, the ESR sample was placed in a styrofoam tube and nitrogen gas at the chosen temperature was passed by the sample. Both the 77 K and the intermediate temperature irradiations of the infrared samples were done with the sample mounted in the metal Dewar. For each of the anneal steps above room temperature, the infrared and ESR samples were removed from their respective Dewars, heated simultaneously in a furnace, and then remounted in the Dewars.

A most important feature of the present investigation is the determination of absolute concentrations of specific defects using the infrared and ESR data. An ESR spin standard consisting of a single crystal of Al_2O_3 doped with Cr^{3+} ions was

obtained from the National Bureau of Standards, Office of Standard Reference Materials. Transfer of the known spin concentration to an unknown quartz sample was accomplished by placing the unknown and standard in the microwave cavity simultaneously, thus eliminating errors due to spectrometer operation, and performing double numerical integrations of the resulting spectra.[26] In the case of the infrared measurements, the expression $N_H = 2.16 \times 10^{16} H\alpha_m$ was used for concentration determinations. Originally presented by Kats,[10] this expression gives the OH^- concentration $N_H(\text{defects/cm}^3)$ in terms of the half-width $H(\text{cm}^{-1})$ and maximum absorption coefficient $\alpha_m(\text{cm}^{-1})$ of the infrared absorption band. A gaussian shape for the absorption curve and an effective charge of p - 0.43 for the oscillator have been assumed.[10] The half-widths of the 3367 cm^{-1} and 3306 cm^{-1} infrared bands were taken to be 8.0 cm^{-1} and 7.4 cm^{-1}, respectively, at 77-80 K where our measurements were performed. Smaller half-widths have been reported by other researchers using higher-resolution instruments.

D. Results

In Fig. 2, the infrared absorption of the unswept Premium Q sample PQ-E10 is shown following each step of an irradiation and thermal anneal sequence. The initial spectrum (Fig. 2a) was obtained from the as-received sample, without prior irradiation. The broad bands at 3200 cm^{-1} and 3300 cm^{-1} have been attributed to intrinsic overtone vibrations of the quartz lattice[10] and, thus, should remain unchanged throughout the sequence depicted in Fig. 2. Additional smaller bands at 3400, 3440, and 3585 cm^{-1} are due to OH^- molecules stabilized in defect configurations that have not yet been identified.[10-14] These latter three bands are very pronounced in Sawyer Electronic Grade material but are barely observable in Sawyer Premium Q material.[14]

The infrared spectrum shown in Fig. 2b was obtained after sample PQ-E10 was irradiated at 77 K and maintained at this low temperature. This treatment

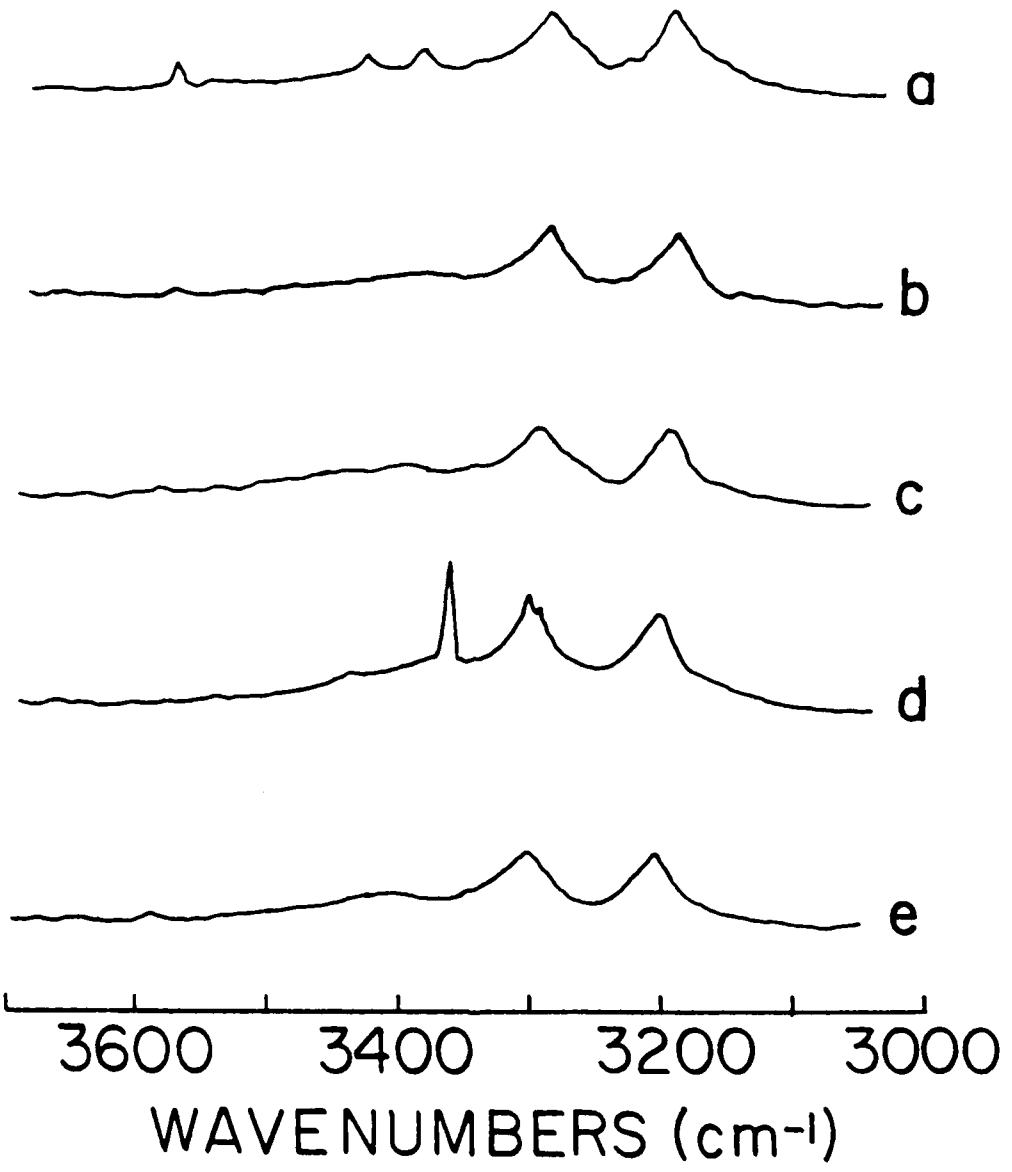

Figure 2. Infrared absorption spectra from unswept Premium Q sample PQ-E10 after each step in the following sequence: (a) as-received, without prior irradiation, (b) irradiation at 77 K, (c) anneal to room temperature, (d) irradiation at room temperature, and (e) reirradiation at 77 K.

greatly reduced the three OH^- bands initially present in the sample and left only the two intrinsic bands. Warming the sample to room temperature (Fig.2c) failed to restore the OH^- bands at 3400, 3440, and 3585 cm^{-1}. As shown in Fig. 2d, a room temperature irradiation introduces the two bands at 3306 and 3367 cm^{-1}. The 3306 cm^{-1} band is a shoulder on the side of the intrinsic 3300 cm^{-1} band and is sometimes difficult to resolve in relatively pure samples. As a final step in the irradiation and anneal sequence, the infrared spectrum (Fig. 2e) of sample PQ-E10 was obtained after irradiation at 77 K. This second irradiation at 77 K eliminated the bands at 3306 and 3367 cm^{-1}, following their introduction by the room temperature irradiation.

An ESR sample labeled PQ-E10 was taken from a position in the quartz bar adjacent to the infrared sample PQ-E10. This unswept ESR sample was subjected to the same irradiation and thermal anneal sequence as the infrared sample; the results being shown in Fig. 3. Examination of the as-received sample (Fig. 3a) revealed no ESR spectra. Irradiation at 77 K produced a few very weak unidentified ESR spectra (Fig. 3b), but these disappeared after warming the sample to room temperature (Fig. 3c). The irradiation at room temperature introduced an intense set of closely-spaced ESR lines extending over a 30 G region when the magnetic field is aligned along the crystal's c-axis. This spectrum, shown in Fig. 3d, is centered at $g_c = 2.0183$ and has been assigned by previous investigators to the Al-hole centers.[15,17,20] The second irradiation at 77 K further enhanced the number of Al-hole centers (Fig. 3e)

The other half of the quartz bar from which the unswept samples PQ-E10 were taken had been swept by Sawyer. An infrared sample and an adjacent ESR sample, both labeled PQ-F12, were cut from this swept portion of the original bar. They then were subjected to the same irradiation and thermal anneal sequence as the unswept samples.

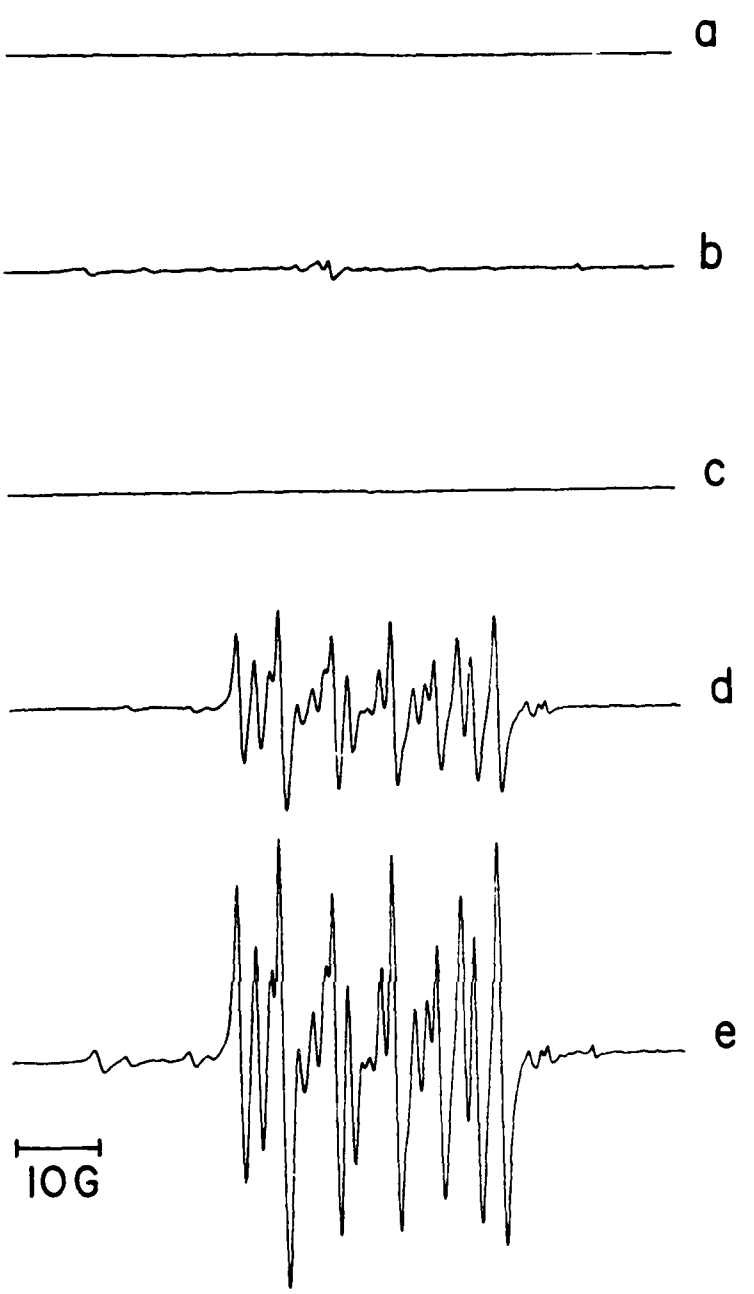

Figure 3. ESR spectra from unswept Premium Q sample PQ-E10 after each step in the following sequence: (a) as-received, without prior irradiation, (b) irradiation at 77 K, (c) anneal to room temperature, (d) irradiation at room temperature, and (e) reirradiation at 77 K.

The infrared absorption results for the swept sample PQ-F12 are shown in Fig. 4. The two bands at 3306 and 3367 cm^{-1} as well as the smaller bands at 3400, 3440, and 3585 cm^{-1} are present prior to any irradiation (Fig. 4a). Irradiation at 77 K destroys all of these bands (Fig. 4b), but warming the sample to room temperature (Fig. 4c) restored the 3306 and 3367 cm^{-1} bands and partially restored the additional weaker bands. Irradiation at room temperature (Fig. 4d) caused no change in the infrared spectrum while the second irradiation at 77 K destroyed all the bands (Fig. 4e) in a manner similar to the first irradiation at 77 K.

The ESR spectra obtained from the swept sample PQ-F12 following each step of the irradiation and anneal sequence are shown in Fig. 5. No signals were observed prior to irradiation (Fig. 5a). The first irradiation at 77 K produced an intense Al-hole center spectrum (Fig. 5b) but nearly all of these centers were destroyed during the anneal to room temperature (Fig. 5c). Additional irradiation at room temperature (Fig. 5d) failed to change the ESR spectrum, while the second irradiation at 77 K produced an intense Al-hole center spectrum (Fig. 5e) very similar to that produced by the first irradiation at 77 K.

The combined concentration of centers giving rise to the 3306 and 3367 cm^{-1} infrared bands along with the concentration of the Al-hole centers were determined for the PQ-E10 and PQ-F12 samples following each step of the irradiation and anneal sequency. These results are given in the first and second columns of Tables I and II. Although not determined explicitly, the concentrations of $A\ell$-M^+ centers (where M^+ represents an alkali ion) given in the third column of Tables I and II were deduced from the Al-hole center data according to the following scheme. The difference in Al-hole center concentration following the first 77 K irradiation and the second 77 K irradiation is taken to represent the initial concentration of $A\ell$-M^+ centers.[22] Since the $A\ell$-M^+ centers are not affected by irradiations below 200 K but are destroyed by irradiations above this temperature,[27] the $A\ell$-M^+ center concentration remains constant for the first three steps of the irradiation and

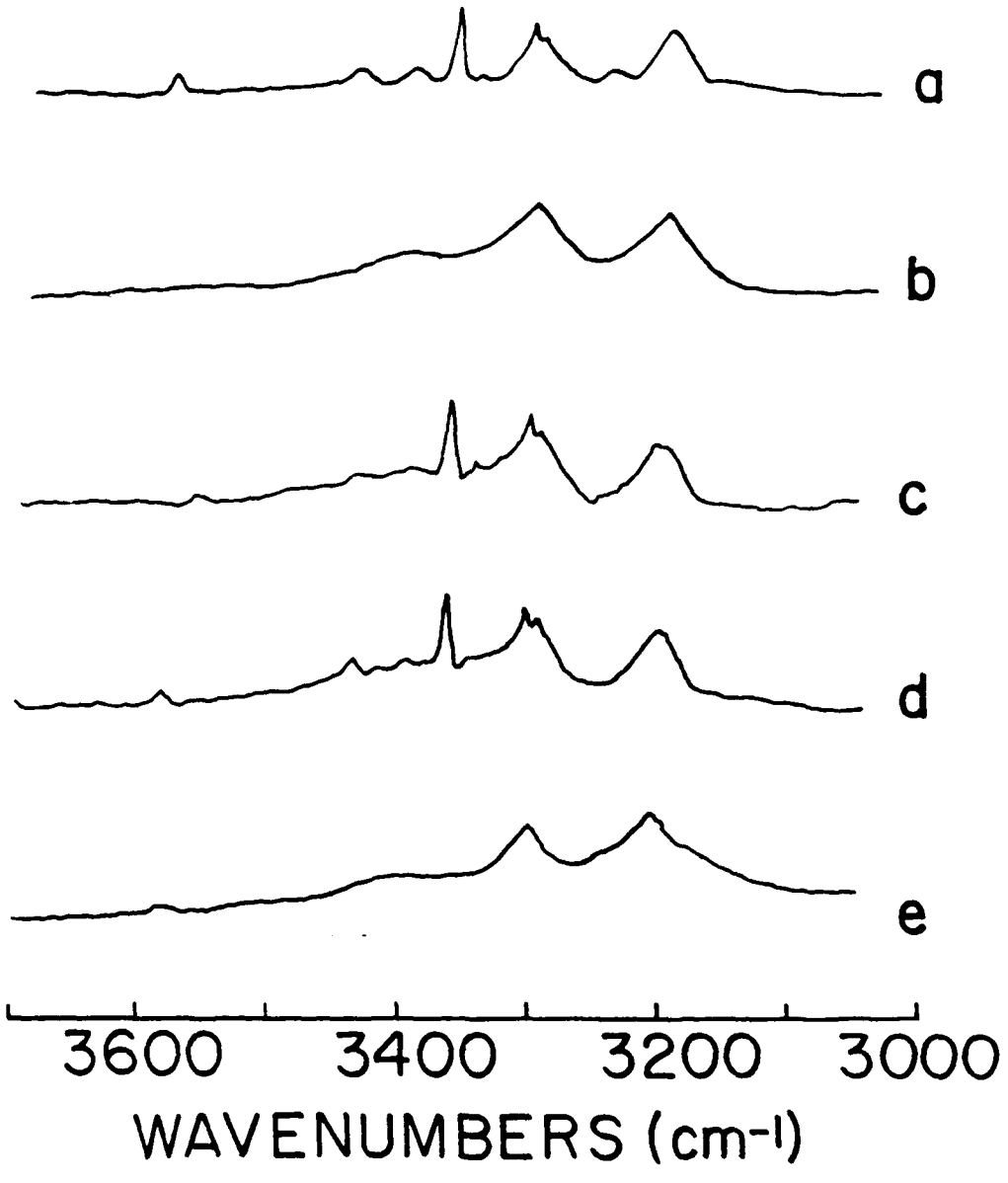

Figure 4. Infrared absorption spectra from Sawyer-swept Premium Q sample PQ-F12 after each step in the following sequence: (a) as-received, without prior irradiation, (b) irradiation at 77 K, (c) anneal to room temperature, (d) irradiation at room temperature, and (d) reirradiation at 77 K.

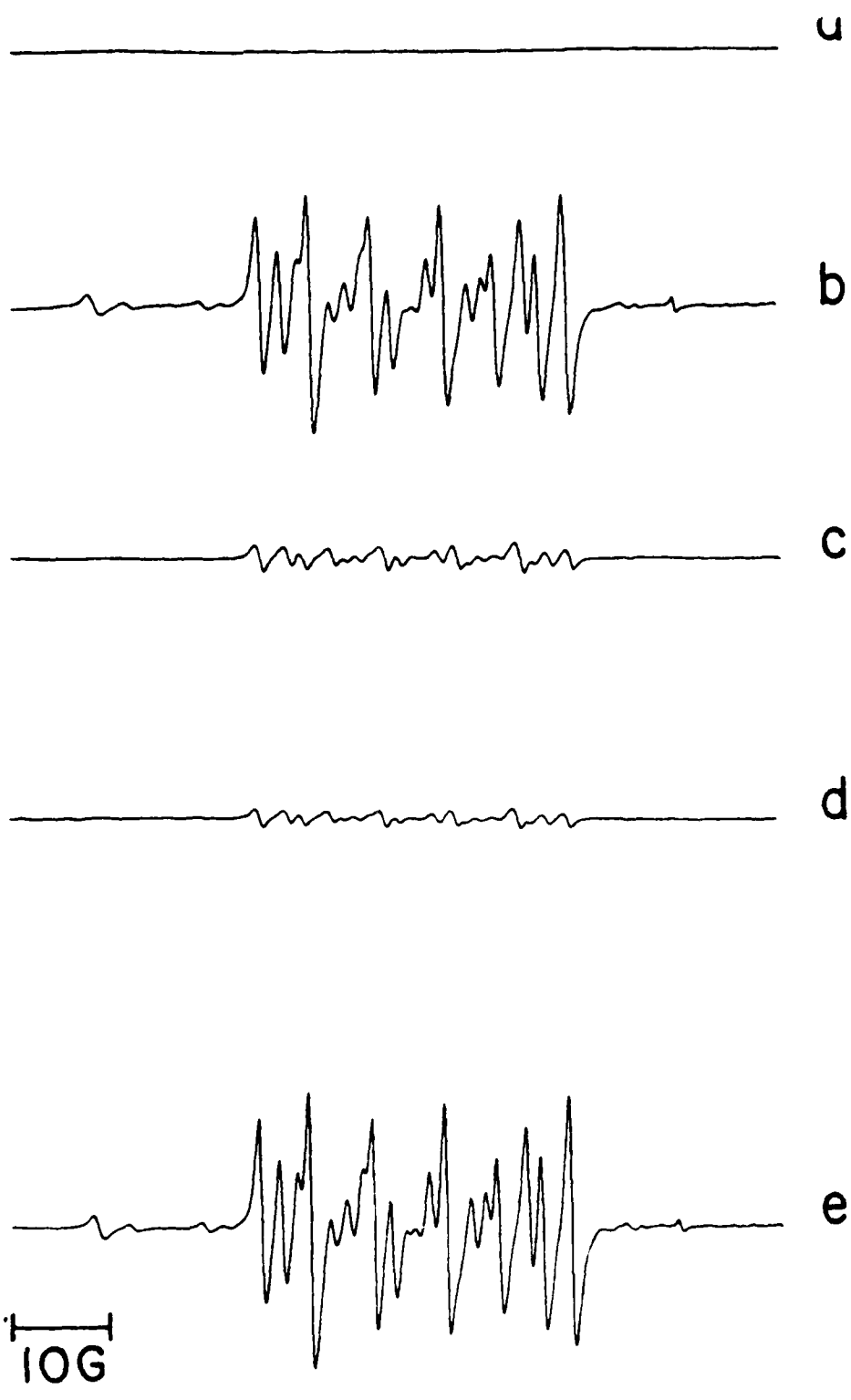

Figure 5. ESR spectra from Sawyer-swept Premium Q sample PQ-F12 after each step in the following sequence: (a) as-received, without prior irradiation, (b) irradiation at 77 K, (c) anneal to room temperature, (d) irradiation at room temperature, and (e) reirradiation at 77 K.

anneal sequence and drops to zero for the last two steps. Finally, the total concentration of all three aluminum-associated defects is given in the fourth column of Tables I and II for each step of the sequence.

Similar infrared and ESR measurements were made on samples cut from additional quartz bars. The concentrations of the various aluminum-associated centers following each step of the irradiation and anneal sequence are given in Tables III-VIII for these latter samples. Results for the unswept sample PQ-A20 and the swept sample PQ-D1, both Sawyer Premium Q material, are presented in Table III and IV, respectively. Tables V and VI contain the results from unswept sample EG-C20 and swept sample EG-F20, both Sawyer Electronic Grade material. The PQ-D and EG-F lumbered bars were swept by Sawyer. Finally, for comparison, the unswept sample SQ-A1 described in Table VII was taken from a bar of Toyo Supreme Q material. Sample SQ-A2 was cut from an adjacent position in the same Toyo bar and then swept in a hydrogen atmosphere at Oklahoma State University prior to obtaining the data presented in Table VIII. In our ESR and infrared absorption experiments, we have been unable to differentiate between sweeping in hydrogen and sweeping in air. Thus, we will use the notation hydrogen-swept in the remainder of the report to refer to sweeping in either atmosphere.

Since the low temperature irradiations did not always destroy all of the $Al\text{-}OH^-$ centers in these latter samples (apparently because of insufficient radiation doses), the $Al\text{-}M^+$ center concentrations were determined by taking the difference in the sum of the $Al\text{-}OH^-$ and Al-hole center concentrations following the first and second 77 K irradiations. In the case of sample PQ-D1 and EG-F20 where the second 77 K irradiation gave a larger concentration of $Al\text{-}OH^-$ plus Al-hole centers than the first 77 K irradiation, the $Al\text{-}M^+$ center concentration is arbitrarily set equal to zero.

TABLE I. Concentration of the aluminum-associated defects in unswept Sawyer Premium Q sample PQ-E10. Units are 10^{16} centers/cm^3.

	Al-OH^-	$[Al_{e+}]^o$	Al-M^+	TOTAL
As-received	0	0	40.2	40.2
1st 77 K irradiation	0	0.2	40.2	40.4
Anneal to room temperature	0	0	40.2	40.2
Room temperature irradiation	13.8	15.2	0	29.0
2nd 77 K irradiation	0	40.4	0	40.4

TABLE II. Concentration of the aluminum-associated defects in Sawyer-swept Premium Q sample PQ-F12. Units are 10^{16} centers/cm^3.

	Al-OH^-	$[Al_{e+}]^o$	Al-M^+	TOTAL
As-received	11.4	0	6.0	17.4
1st 77 K irradiation	0	12.9	6.0	18.9
Anneal to room temperature	10.6	1.5	6.0	18.1
Room temperature irradiation	10.3	1.2	0	11.5
2nd 77 K irradiation	0	18.9	0	18.9

TABLE III. Concentration of the aluminum-associated defects in unswept Sawyer Premium Q sample PQ-A20. Units are 10^{16} centers/cm^3.

	Al-OH^-	$[Al_{e+}]^o$	Al-M^+	TOTAL
As-received	0	0	3.9	3.9
1st 77 K irradiation	0	0	3.9	3.9
Anneal to room temperature	0	0	3.9	3.9
Room temperature irradiation	2.8	0.4	0	3.2
2nd 77 K irradiation	0	3.9	0	3.9

TABLE IV. Concentration of the aluminum-associated defects in Sawyer-swept Premium Q sample PQ-D1. Units are 10^{16} centers/cm^3.

	Al-OH^-	$[Al_{e+}]^o$	Al-M^+	TOTAL
As-received	9.3	0	0	9.3
1st 77 K irradiation	0	15.1	0	15.1
Anneal to room temperature	8.4	1.7	0	10.1
Room temperature irradiation	9.2	1.0	0	10.2
2nd 77 K irradiation	0	14.6	0	14.6

TABLE V. Concentration of the aluminum-associated defects in unswept Sawyer Electronic Grade sample EG-C20. Units are 10^{16} centers/cm^3.

	Al-OH^-	$[Al_{e+}]^o$	Al-M^+	TOTAL
As-received	0	0	41.3	41.3
1st 77 K irradiation	0	2.9	41.3	44.2
Anneal to room temperature	1.4	0.7	41.3	43.4
Room temperature irradiation	32.1	5.1	0	37.2
2nd 77 K irradiation	5.6	38.6	0	44.2

TABLE VI. Concentration of the aluminum-associated defects in Sawyer-swept Electronic Grade sample EG-F20. Units are 10^{16} centers/cm^3.

	Al-OH^-	$[Al_{e+}]^o$	Al-M^+	TOTAL
As-received	N.A.[1]	0	0	N.A.[1]
1st 77 K irradiation	3.3	20.4	0	23.7
Anneal to room temperature	13.0	2.1	0	15.1
Room temperature irradiation	11.9	4.9	0	16.8
2nd 77 K irradiation	0	20.0	0	20.0

[1]N.A. (not available)

TABLE VII. Concentration of the aluminum-associated defects in unswept Toyo Supreme Q sample SQ-A1. Units are 10^{16} centers/cm^3.

	$Al\text{-}OH^-$	$[Al_{e+}]^o$	$Al\text{-}M^+$	TOTAL
As-received	0	0	32.3	32.3
1st 77 K irradiation	0	0.6	32.3	32.9
Anneal to room temperature	0	0.3	32.3	32.6
Room temperature irradiation	14.8	22.8	0	37.6
2nd 77 K irradiation	4.5	28.4	0	32.9

TABLE VIII. Concentration of the aluminum-associated defects in hydrogen-swept Toyo Supreme Q sample SQ-A2. Units are 10^{16} centers/cm^3.

	$Al\text{-}OH^-$	$[Al_{e+}]^o$	$Al\text{-}M^+$	TOTAL
As-received	35.1	0	0	35.1
1st 77 K irradiation	7.5	31.3	0	38.8
Anneal to room temperature	28.4	3.9	0	32.3
Room temperature irradiation	27.7	3.9	0	31.6
2nd 77 K irradiation	5.0	33.8	0	38.8

In all of the unswept samples examined, only a few of the Al-hole centers and none of the 3306 and 3367 cm^{-1} infrared bands are produced by the initial 77 K irradiation, but they appear with significant intensity after the subsequent room temperature irradiation. A second 77 K irradiation further enhances the Al-hole center ESR spectrum but destroys the two infrared bands. In order to determine the critical temperature range above which these two infrared bands and the Al-hole center ESR spectrum are initially enhanced by radiation, several unswept samples were subjected to a series of irradiations at progressively higher temperatures between 77 K and 300 K. The growth of the 3367 cm^{-1} infrared band and the Al-hole center ESR spectrum are shown in Fig. 6 for the unswept Sawyer Premium Q sample PQ-E11 and the unswept Toyo Supreme Q sample SQ-A3. In this figure, the infrared samples were immediately measured at 77 K following each intermediate temperature irradiation while the ESR samples were re-irradiated at 77 K each time to insure filling all electron traps before measuring the Al-hole center ESR spectrum.

As shown in Fig. 7, an unswept sample irradiated at room temperature can be restored to its as-received state by simply heating to the 500-650 K region. Unswept samples PQ-E10 and SQ-A1 were first irradiated at room temperature and then sequentially heated to the indicated higher temperatures where they were held for 15 min before being returned to 77 K. Each infrared data point (sum of the 3306 and 3367 cm^{-1} bands) in Fig. 7 was taken immediately upon returning the sample to 77 K, whereas the taking of each ESR data point in Fig. 7 was preceded by a 77 K irradiation. Thus, the infrared data represents a simple pulsed anneal experiment describing the thermal stability of the two infrared bands; while the ESR data does not necessarily provide information about the thermal stability of the Al-hole center but rather

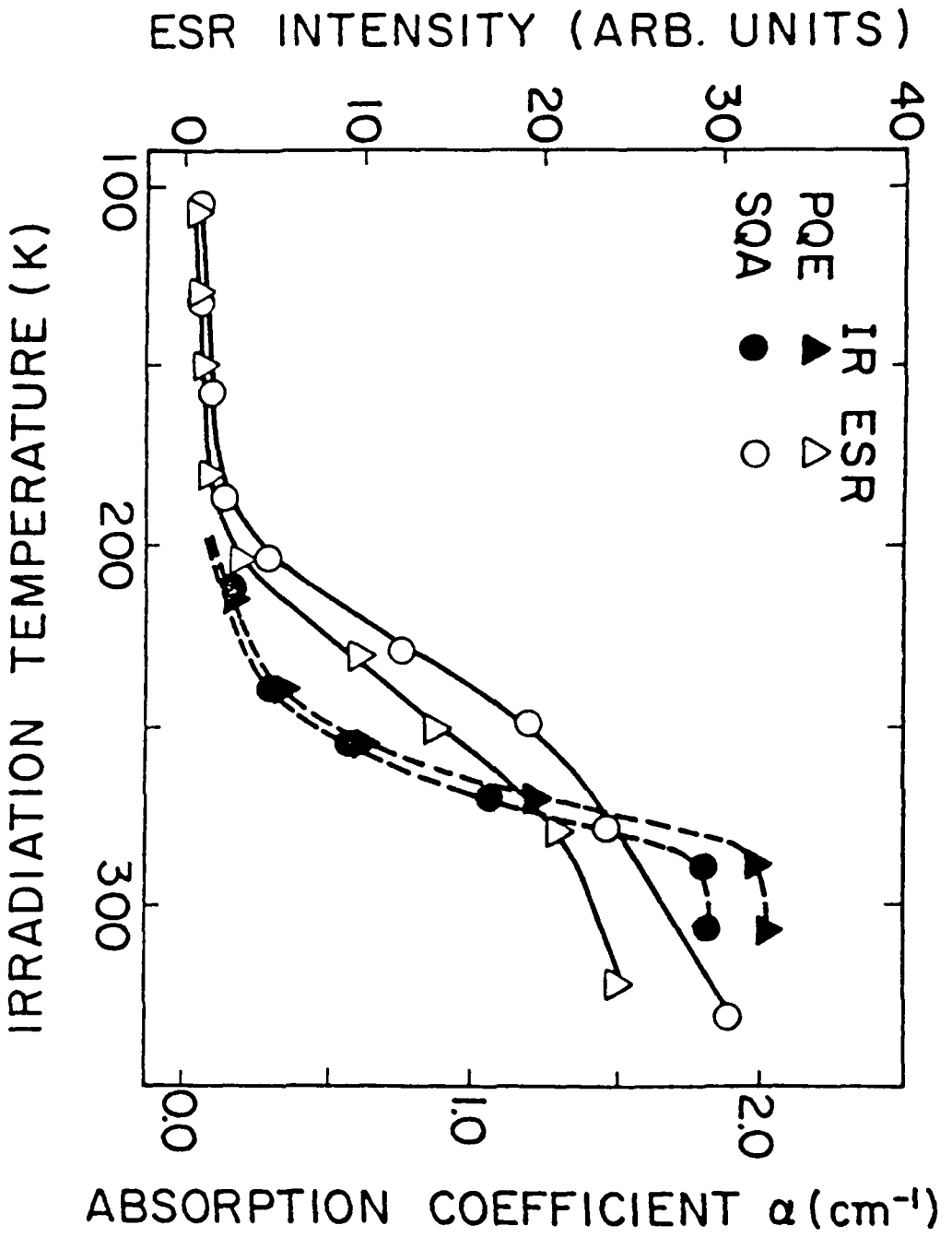

Figure 6. Production of the 3367 cm^{-1} infrared band and the $[Al_{e+}]^{\circ}$ center ESR spectrum as a function of irradiation temperature for the unswept Sawyer Premium Q sample PQ-E11 and the unswept Toyo Supreme Q sample SQ-A3.

Figure 7. Effect of high temperature annealing on the stability of the 3306 and 3367 cm^{-1} infrared bands and on the production of the $[Al_{e+}]^{\circ}$ center ESR spectrum by 77 K irradiation. The data are from unswept Sawyer Premium Q sample PQ-E19, Sawyer-swept Premium Q sample PQ-F12, and unswept Toyo Sumpreme Q sample SQ-A1.

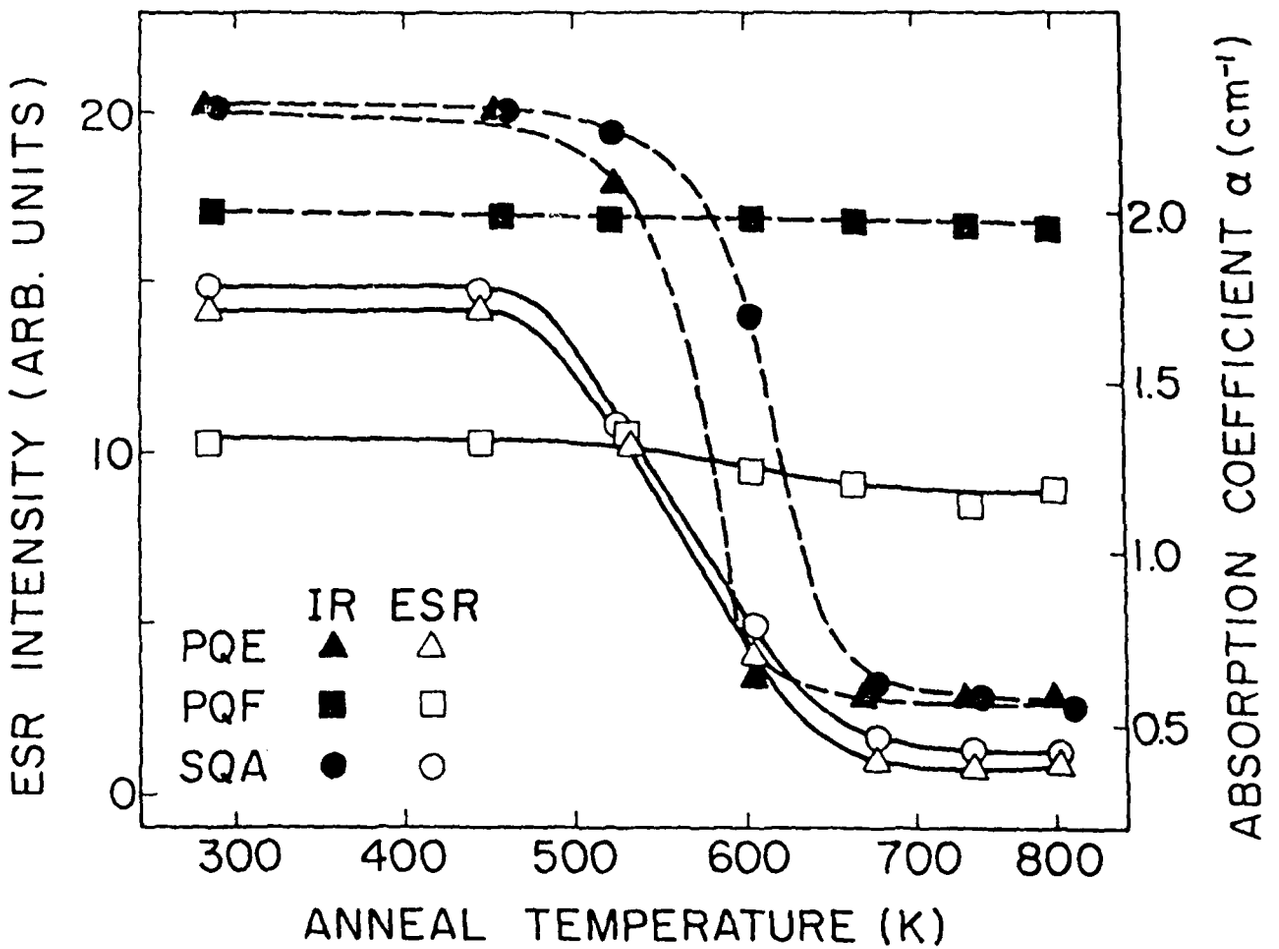

indicates the concentration of Al-hole centers that can be generated by a 77 K irradiation. The results in Fig. 7 show that the ability to enhance the Al-hole center concentration by a second 77 K irradiation in unswept samples disappears in the same temperature region as the two infrared bands. Also shown in Fig. 7 are the results of similar infrared and ESR measurements on the swept sample PQ-F12. In direct contrast to the unswept samples, no significant changes in the 500-650 K temperature region were observed for the swept sample.

E. Discussion

The present experimental investigation has provided information about the role of aluminum (via its need for charge compensation) in the radiation response of high-quality synthetic quartz. Specifically, we have (1) made absolute concentration measurements of aluminum-associated defects in quartz as a function of sample treatment; (2) provided conclusive evidence supporting the $Al\text{-}OH^-$ model for the 3306 and 3367 cm^{-1} infrared bands; (3) further verified that the radiation-induced mobility of interstitials is a fundamental radiation response of quartz, while demonstrating that aluminum is a dominant interstitial trap; and (4) compared the radiation response of high-quality quartz obtained from two independent sources (Sawyer and Toyo).

In the present investigation, we did not monitor the $Al\text{-}M^+$ centers directly but inferred their presence from the absence of $Al\text{-}OH^-$ and Al-hole centers. It is important to note that this is not a limitation of our results since the recent acoustic loss measurements of Doherty et al.[28], where the $Al\text{-}Na^+$ centers were observed directly, strongly support our method of accounting for aluminum ions not found in the form of $Al\text{-}OH^-$ or Al-hole centers.

1. Absolute Concentration Measurements

The results presented in Tables I-VIII suggest that substitutional aluminum ions in high-quality quartz have either interstitial hydrogen ions, radiation-induced holes, or interstitial alkali ions as charge compensators. The absolute concentration of aluminum ions possessing a specific compensator varies in a systematic manner, and depends on what stage the sample is at in the irradiation and anneal sequence and on whether the sample has been swept or not. As-received unswept samples have only $Al\text{-}M^{+}$ centers whereas as-received hydrogen-swept samples have primarily $Al\text{-}OH^{-}$ centers. Sample PQ-712 appears to be an exception to this last statement but that is simply because the sweeping was not completed. The 1st 77 K irradiation eliminates $Al\text{-}OH^{-}$ centers and produces Al-hole centers in hydrogen-swept samples, but does not significantly affect unswept samples. Returning a sample, either hydrogen-swept or unswept, to room temperature following the initial 77 K irradiation restores it to near the as-received condition. Room temperature irradiation always leaves $Al\text{-}OH^{-}$ centers and Al-hole centers; the relative ratio of the concentrations of the two centers depending on factors not yet identified. Only Al-hole centers are observed after the 2nd 77 K irradiation in both swept and unswept samples.

If all of the aluminum in a sample can be accounted for either as Al-OH^-, Al-hole, or Al-M^+ centers, then the totals (i.e., the sums of the three centers) for a given sample will remain constant as the sample is cycled through the sequence of irradiations and anneals. Since the data in Tables I-VIII come from two completely independent experiments, ESR and infrared absorption, variations in the totals for a given sample are not unexpected. However, it is satisfying to note that the observed variations are within the expected experimental error (including estimates of random as well as systematic contributions) of 25% to 50%. Among the potential sources of error are (1) the choice of "effective" oscillator strengths for the infrared bands; (2) the possibility that the irradiations were not always saturating the concentration of defects; and (3) the possibility of nonuniformity of aluminum content from the ESR sample to the infrared sample even though they were taken from adjacent positions in the quartz bars.

In the case of samples PQ-E10 and EG-F20, the mass spectroscopy data presented in Reference 22 provides additional confirmation of the aluminum concentrations found in the present investigation. Sample PQ-E3 was reported in the earlier work to have a total aluminum content of 7 μg/g, which is equivalent to a concentration of 41.3×10^{16} cm^{-3}; whereas the present ESR and infrared results (Table I) give a maximum concentration of 40.4×10^{16} cm^{-3} for the aluminum in sample PQ-E10. These two Premium Q samples, PQ-E3 and PQ-E10, are from the same bar, although different locations, and the fortuitously small difference between the mass spectroscopy and ESR-infrared results for the total aluminum concentration can easily be attributed to the nonuniform distribution of the aluminum ions within the quartz bar. Samples EG-E39 and EG-E42 were reported in Reference 22 to have aluminum concentrations

of 3 and 2 μg/g, respectively (i.e., 17.7×10^{16} cm^{-} and 11.8×10^{16} cm^{-3}). Sample EG-F20 is from the same original bar as samples EG-E39 and EG-E42 and should have a similar aluminum content.[22] The ESR and infrared results (Table VI) give concentrations ranging from 15.1×10^{16} cm^{-3} to 23.7×10^{16} cm^{-3} for the aluminum in sample EG-F20. Again, the agreement between the mass spectroscopy and ESR-infrared results as to total aluminum content is reasonable, considering that the EG-E and EG-F samples were from opposite ends of the original bar.

2. Infrared Band Identifications

In the past, Kats,[10] Brown and Kahan,[11] and others[12-14] have suggested that the 3306 and 3367 cm^{-1} infrared absorption bands arise from an $Al-OH^{-}$ center (i.e., on OH^{-} molecule adjacent to a substitutional aluminum). Given the behavior of these two bands as described by previous investigators, this is a conceptually satisfying explanation of their origin and since there is no significant conflicting data, the simple $Al-OH^{-}$ model has not been disputed in the literature. However, despite this general acceptance of the model, conclusive evidence has not yet been presented to directly link the 3306 and 3367 cm^{-1} bands to aluminum. In the case of the paramagnetic Al-hole center, the presence of aluminum is clearly indicated by the resolved aluminum hyperfine interactions in the ESR spectra.[21] There are, of course, no effects analogous to the hyperfine splitting which connect the two infrared bands to aluminum.

In the present investigation, the concentration of defects giving rise to the 3306 and 3367 cm^{-1} infrared bands in hydrogen-swept samples (Tables II, IV, VI, and VIII) is seen to vary inversely with the Al-hole center concentration. Whenever the 3306 and 3367 cm^{-1} bands are intense, the Al-hole center ESR

spectrum is relatively weak, and vice versa. A similar, although not as pronounced, relationship exists for the unswept samples (Tables I, III, V, and VII) during the room temperature and 2nd 77 K irradiations. More precisely stated, the sum of the Al-hole center concentration and the infrared-active-defect concentration remains constant, within experimental error, for a given sample for all cases where the Al-M^+ center concentration is negligible.

The variable temperature irradiation data presented in Fig. 6 and the high-temperature anneal data presented in Fig. 7 provide additional evidence linking aluminum with the 3306 and 3367 cm^{-1} infrared bands. In both cases, the Al-hole center ESR spectrum and the two infrared bands exhibit similar behavior. As shown in Fig. 6, the ESR and infrared spectra are enhanced by irradiation temperatures above 200 K in previously unirradiated, unswept samples. The high-temperature anneal data from unswept samples (Fig. 7) show that the thermal decay of the two infrared bands correlates directly with the disappearance of the ability to enhance the production of Al-hole centers by 77 K re-irradiation. The hydrogen-swept sample shows quite different behavior during the high-temperature anneal (Fig. 7) when compared to the unswept samples, but the correlation between the Al-hole center spectrum and the two infrared bands remains excellent in the case of the hydrogen-swept sample. All of the results in Figs. 6 and 7 are a consequence of the alkali interstitial ions, their presence in the unswept samples and their absence in the hydrogen-swept samples.

There is no doubt that the Al-hole center is aluminum-related and that the Al-hole centers and the 3306 and 3367 cm^{-1} infrared bands are closely related. The nature of the relationship is either correlative or anti-correlative depending on the specific experiment (e.g., sum of the absolute

concentrations, variable temperature irradiations, and high-temperature anneals). Considered as a whole, these results strongly suggest that the 3306 and 3367 cm^{-1} infrared bands in quartz are associated with substitutional aluminum ions, and the simplest such defect would be the $Al\text{-}OH^{-}$ center.

3. Radiation Response Mechanisms

It was recognized early in the study of quartz that the radiation-induced mobility of interstitial cations was an important factor in the radiation response of both natural and synthetic material. O'Brien[16] suggested that the Al-hole center was formed when ionizing radiation removed both an electron and a positive interstitial ion (either alkali or hydrogen) from the vicinity of the substitutional aluminum. Kats[10] and Brown and Kahan[11] explained the production of the 3306 and 3367 cm^{-1} infrared absorption bands by irradiation in terms of the retrapping of interstitial hydrogen ions at aluminum sites after an initial radiation-induced release of interstitial alkali ions from the aluminum sites and hydrogen from other trapping sites. King and Sander[1] have proposed that the transient frequency shifts observed in quartz oscillators result from the radiation-induced motion of interstitial hydrogen away from aluminum sites followed immediately by a thermally-induced diffusion of the hydrogen back to the aluminum. The more recent work of Markes and Halliburton[22] and Sibley et al.[14] has shown that the interstitial hydrogen ion can be displaced by irradiation at any temperature whereas interstitial alkalis only become mobile when the irradiation temperature is above 200 K.

The results from the present study strongly support the work of the earlier investigators and thus further verify the following description of the response of high-quality synthetic quartz to ionizing radiation. The aluminum in as-received unswept quartz normally is only in the form of $Al\text{-}M^{+}$

centers and irradiation at 77 K has essentially no effect on such samples. At this low temperature, the interstitial alkali ion can not be removed from the aluminum site and this, in turn, prevents hydrogen ions released by the radiation from being trapped at the aluminum site. The hydrogen ions, instead, become trapped at other unidentified sites.[22] Irradiation of the unswept samples above 200 K gives quite different results since there is then sufficient thermal energy available to allow the radiation-induced dissociation of the $Al\text{-}M^+$ centers. As the interstitial alkali ions are removed from the aluminum sites, holes and interstitial hydrogen ions are trapped by the aluminum to form Al-hole centers and $Al\text{-}OH^-$ centers, respectively. Annealing the unswept samples above 600 K destroys the Al-hole centers and $Al\text{-}OH^-$ centers and restores the $Al\text{-}M^+$ centers.

In the case of hydrogen-swept quartz, the interstitial alkali ions have been replaced by interstitial hydrogen ions and, before irradiation, all of the aluminum is in the form of $Al\text{-}OH^-$ centers. Irradiation at 77 K dissociates the OH^- molecules and allows the hydrogen to move away from the aluminum site. The hydrogen then acts as an electron trap while the aluminum becomes a hole trap, i.e., hydrogen atoms[29,30] and Al-hole centers are formed. If the temperature of the sample is raised above 130 K following the 77 K irradiation, the hydrogen atoms thermally decay and the Al-hole center concentration decreases significantly.[22] Irradiation of the hydrogen-swept samples at room temperature also dissociates the OH^- molecules and moves the hydrogen away from the aluminum but the lack of stable trapping sites at this higher temperature forces many of the hydrogens to return to the aluminum ions. During the short period of time the hydrogen is displaced from the aluminum, a hole may be trapped by the aluminum in the form of Al-hole centers. The return of the hydrogen converts the Al-hole centers back into $Al\text{-}OH^-$

centers. Thus, in hydrogen-swept samples, the steady state concentration of Al-hole centers remaining after the room temperature irradiation is significantly reduced from the value attained during irradiation and it is also considerably less than the steady state concentration produced by a 77 K irradiation.

Within the general description of the response of quartz to ionizing radiation, a number of questions remain unanswered. Thus far, no conclusive experimental evidence has been presented regarding the identity of the electron traps in quartz. When hydrogen-swept samples are irradiated and maintained below 125 K, hydrogen atoms[29,30] are believed to play the role of electron traps.[31] In the case of unswept quartz and hydrogen-swept quartz above 125 K, the data presented in this report along with additional data to be reported,[31] although not conclusive, suggest that the interstitial alkali ions play a direct role in forming stable electron traps. Also, the radiation-induced dissociation mechanisms for the $Al\text{-}OH^-$ centers and the $Al\text{-}M^+$ centers are not well understood. They appear to be quite distinct mechanisms, as illustrated by their significantly different temperature dependences, and our preliminary evidence suggests they are based on electronic excitation and thermal excitation, respectively.

4. Comparison of Quartz

The quality of synthetic quartz samples, as measured by the total aluminum content, can vary significantly. In the present investigation, four Premium Q and two Electronic Grade samples from Sawyer were examined and the aluminum content varied from 1.5 ppm for sample PQ-A20 to 15.3 ppm for sample PQ-E10. These aluminum content values are based on the number of silicon sites ($1 \text{ ppm} = 2.65 \times 10^{16} \text{ Si/cm}^3$) and are taken from the concentration of Al-hole

centers following the 2nd 77 K irradiation, as given in Tables I-VIII. It is interesting to note the order of magnitude range in aluminum content for Premium Q material. In fact, the Electronic Grade samples had aluminum contents that fell within the range of values for the Premium Q material. A number of reasons exist for the observed variations in aluminum content in synthetic quartz and include (a) the variation in aluminum content of the natural quartz used as the nutrient material in the growth process; (b) the hydrothermal growth conditions in the autoclave, i.e., thermal gradients, mineralizer, etc.; and (c) the quality and orientation of the seed crystal.

Since samples from only one Toyo bar were examined, it is impossible to generalize about the aluminum content of Toyo quartz. However, the one bar yielded samples SQ-A1 and SQ-A2 with 10.7 ppm and 12.8 ppm values, respectively, for aluminum content and these fall within the range of values for the Sawyer samples. Thus, at this time, there is no reason to expect the Toyo material to be significantly better or worse than Sawyer material, at least in regard to impurity content.

Finally, as shown in Figs. 6 and 7 and Tables I-VIII, the Sawyer and Toyo quartz exhibit nearly identical radiation responses. This consistency in material behavior for samples obtained from widely separated sources and possibly grown under differing conditions strongly suggests that we are observing the fundamental (i.e., universal) response of high quality aluminum-containing quartz to ionizing radiation.

F. Summary

The present investigation has made use of infrared absorption and ESR measurement techniques to monitor the absolute concentrations of the various compensated aluminum centers in a variety of high quality synthetic quartz samples. When these results are coupled with the work of previous investigators, a consistent picture of the role of aluminum in the radiation response of quartz emerges and can be

summarized by the following statements:

(1) Aluminum in as-received unswept quartz is primarily in the form of $Al-M^+$ centers.

(2) Aluminum in as-received hydrogen-swept quartz is primarily in the form of $Al-OH^-$ centers.

(3) $Al-OH^-$ centers are converted to Al-hole centers by irradiation at 77 K.

(4) $Al-M^+$ centers are not affected by irradiation at 77 K.

(5) $Al-M^+$ centers are converted into $Al-OH^-$ and Al-hole centers by irradiation at temperatures above 200 K. The ratio of the resulting $Al-OH^-$ and Al-hole centers evidently depends on the types of electron traps present in the sample.

(6) In unswept quartz, $Al-OH^-$ centers are converted into $Al-M^+$ centers by annealing above 600 K.

(7) In hydrogen-swept quartz, $Al-OH^-$ centers are not affected by annealing above 800 K.

Significant questions still remain concerning the identity of electron traps and the nature of the radiation-induced dissociation mechanisms for the $Al-OH^-$ and $Al-M^+$ centers. Also, the fundamental question of why the aluminum in as-grown quartz much prefers to be in the form of $Al-M^+$ centers as opposed to $Al-OH^-$ centers has not been answered.

III. ACOUSTIC LOSS AND ELECTROLYSIS

A. Introduction

Substitutional Al^{3+} is present in all quartz[32] and requires charge compensation. Examples of such charge compensators are interstitial Li^+ or Na^+ ions, or holes or protons at an oxygen ion adjacent to the aluminum. The proton forms an OH^- molecule which is infrared active.[32,10] The $Al-Na^+$ defect is responsible for the acoustic loss peak observed near 50 K in 5 MHz 5th overtone AT-cut crystals.[33] Irradiation at room temperature destroys the $Al-Na^+$ centers [4,28] and this is responsible for

much of the steady state frequency offset. Recent work at Oklahoma State University has shown that the alkali ions become mobile under irradiation only if the temperature is greater than 200 K.[14,22,28] Following a room temperature irradiation, either a hole which can be observed by ESR techniques or a proton is found trapped on an oxygen adjacent to the Al^{3+}. The interstitial alkali ions are usually in the relatively large c-axis channels and at high temperatures can move along the channel under an applied electric field. King,[4] and later Kats[10] and Fraser,[33] used this technique to "sweep" hydrogen and specific alkalis into the sample. Sweeping hydrogen in to replace the alkalis has been shown to improve the radiation hardness of quartz oscillators.[7]

The identification of both growth and radiation-induced defects which affect the performance of quartz resonators is an important part of our project. Recently, using sweeping, IR absorption and acoustic loss measurements Martin and Doherty[34] reported that the $Al\text{-}OH^-$ center does not have an acoustic loss peak at temperatures below 370 K. They also reported that irradiation of both unswept and H_2- swept Premium Q quartz resonator blanks produced acoustic loss peaks at 25 K and 100 K and a broad loss peak between 125 K and 165 K. King and Sander[1] had earlier reported the two higher temperature peaks and had suggested that they were caused by the Al-hole center. The 25K peak had also been observed earlier and was attributed to changes in the interaction between the resonant vibration of the blank and the thermal phonons.[9] We report here an isochronal anneal study of these three loss peaks which shows that all three peaks are associated with the Al-hole center. We also compare the acoustic loss spectrum of unswept and Li-swept Premium Q material.

B. Experimental Procedure

All samples for this study were cut from an unswept pure Z growth Sawyer Premium Q bar of cultured quartz that has been given an in-house designation PQ-E. Samples from this bar have been extensively studied at Oklahoma State University using

ESR,[22,32] IR,[32,34] and acoustic loss[34] techniques. All of these investigations show that the bar is of high quality but that it contains somewhat more aluminum (10-15 ppm) than the average Premium Q material (5-8 ppm). Consequently, aluminum-related effects are more readily observed.

5 MHz 5th overtone AT-cut plano convex resonator blanks of the Warner[35] design were fabricated for this study by K&W Mfg., Prague, OK. The acoustic loss, Q^{-1}, of the resonator blanks was measured by the log decrement method from 5 to 300 K. The measurements were made in a variable temperature helium Dewar with the blanks mounted in a gap holder similar to the one described by Fraser.[9] The blank was driven for 10 ms at its series resonant frequency and then allowed to freely decay. The decaying rf signal was detected with a superheterodyne detector and displayed on a variable persistence storage oscilloscope. The exponential decay times were measured using a window detector to gate a digital timer.

Electrolysis, or sweeping, was carried out at temperatures of 470-480°C in a controlled atmosphere system. This system allowed the use of H_2, D_2, or gettered N_2 atmospheres, or an oil-diffusion-pumped vacuum of approximately 2×10^{-6} Torr. For the acoustic loss studies, the AT-cut resonator blanks were directly swept. Vapor-deposited Au electrodes were used. For the Li sweeping runs, LiCl was vapor deposited on the sample surface and then an Au electrode was deposited over the LiCl layer. The Li electrolysis was carried out in a vacuum better than 5×10^{-6} Torr.

Irradiations were carried out at room temperature using 1.7 MeV electrons from a Van de Graaff accelerator. Typical doses were approximately 2000 J/cm^3 ($\sim 10^8$ rads). This dose is not expected to produce significant knock-on damage, but it has been shown to saturate the Al-related defects. The production of Al-OH^- centers by the irradiation was measured by a liquid nitrogen temperature polarized infrared scan on the resonator blank.

C. Results and Discussion

Figure 8 compares the current-versus-time curves for typical H_2 and Li sweeping runs. The component of the applied field parallel to the c axis is 35 V/cm for the Li sweep and 1500 V/cm for the H_2 sweep. In the H_2 case, the large initial current and subsequent decay is most likely caused by the alkalis being removed from the sample and the low final current is most likely protons being swept through the lattice. Since Li ions are being supplied from the LiCl film at the positive electrode, the current remains nearly constant in the Li sweeping runs. Infrared absorption scans show that no Al-OH^- centers are present in the Li-swept sample. Figure 9 compares the acoustic loss, Q^{-1}, versus temperature spectra for unswept, H_2- swept, and Li- swept resonators fabricated from the PQ-E bar. The Al-Na^+ loss peak near 50 K is absent in both of the swept resonators. We do not see any loss peaks caused by the Al-Li^+ center. Evidently the coupling of this center to the AT thickness shear mode is much weaker than that of the Al-Na^+ center. An earlier comparison[15] of H_2- and D_2- swept PQ-E resonators showed that the Al-OH^- center does not have loss peaks at temperatures below 370 K.

Recently, Martin and Doherty[34] reported that irradiation of unswept and H_2-swept PQ-E resonator blanks at room temperature produced loss peaks at 25 K and 100 K and a broad loss between 125 and 165 K. The peaks were much larger in the unswept material than in the H_2- swept blank. The room temperature irradiation also removed the Al-Na^+ loss peak which was present initially in the unswept blank. King and Sander[1] have previously observed the peak at 100 K and the broad loss between 125 K and 165 K. They attributed these loss peaks to the Al-hole center. Martin and Doherty suggested that the 25 K peak is also due to the Al-hole center. Figure 10 shows the Q^{-1} vs temperature spectrum for the Li-swept resonator blank in the as-swept condition and after a room temperature irradiation. The radiation-induced peaks are in excellent agreement with the earlier results on an unswept blank.

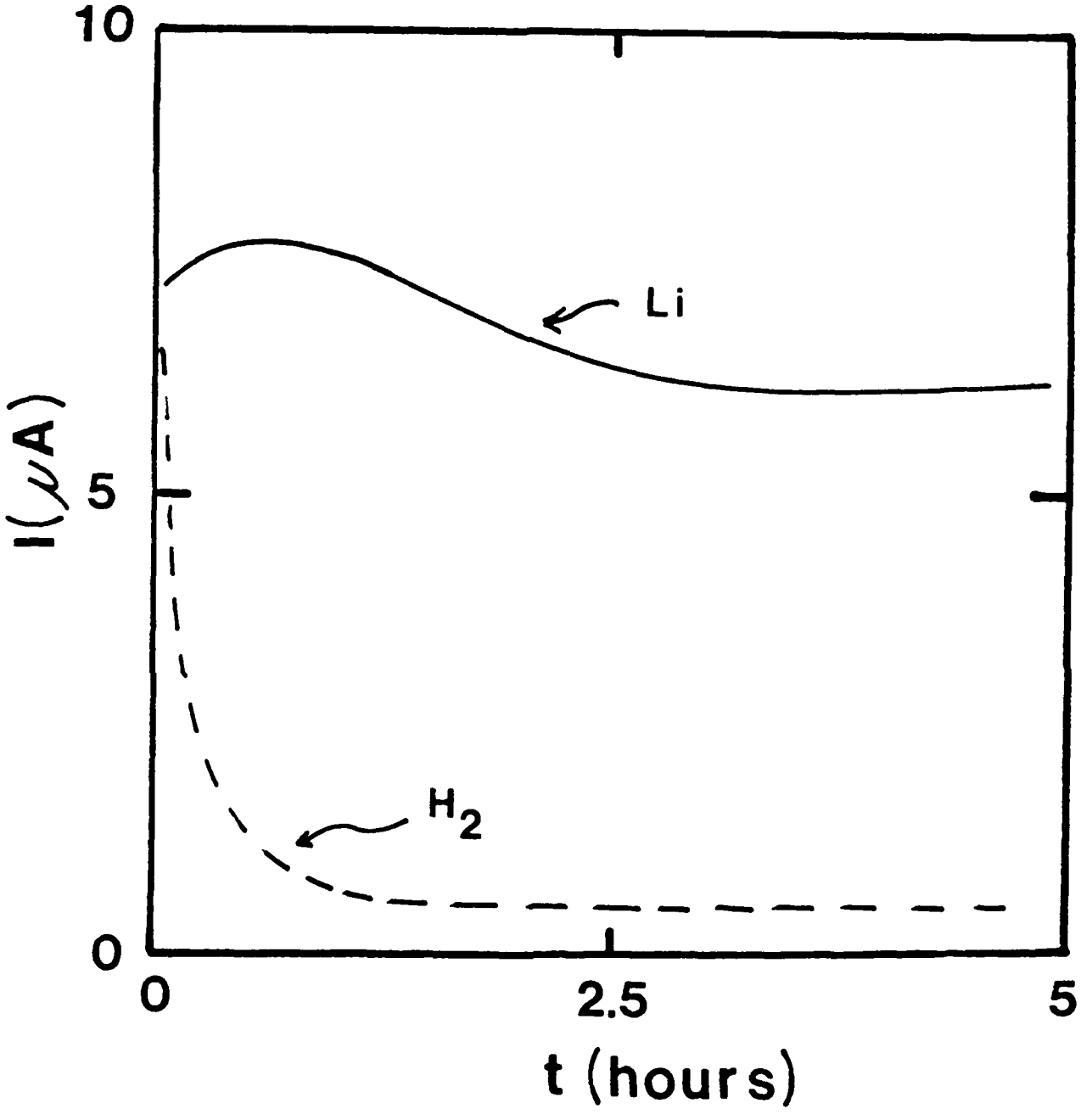

Figure 8. The current-versus-time curves are shown for lithium and hydrogen electrolysis of PQ-E series resonator blanks.

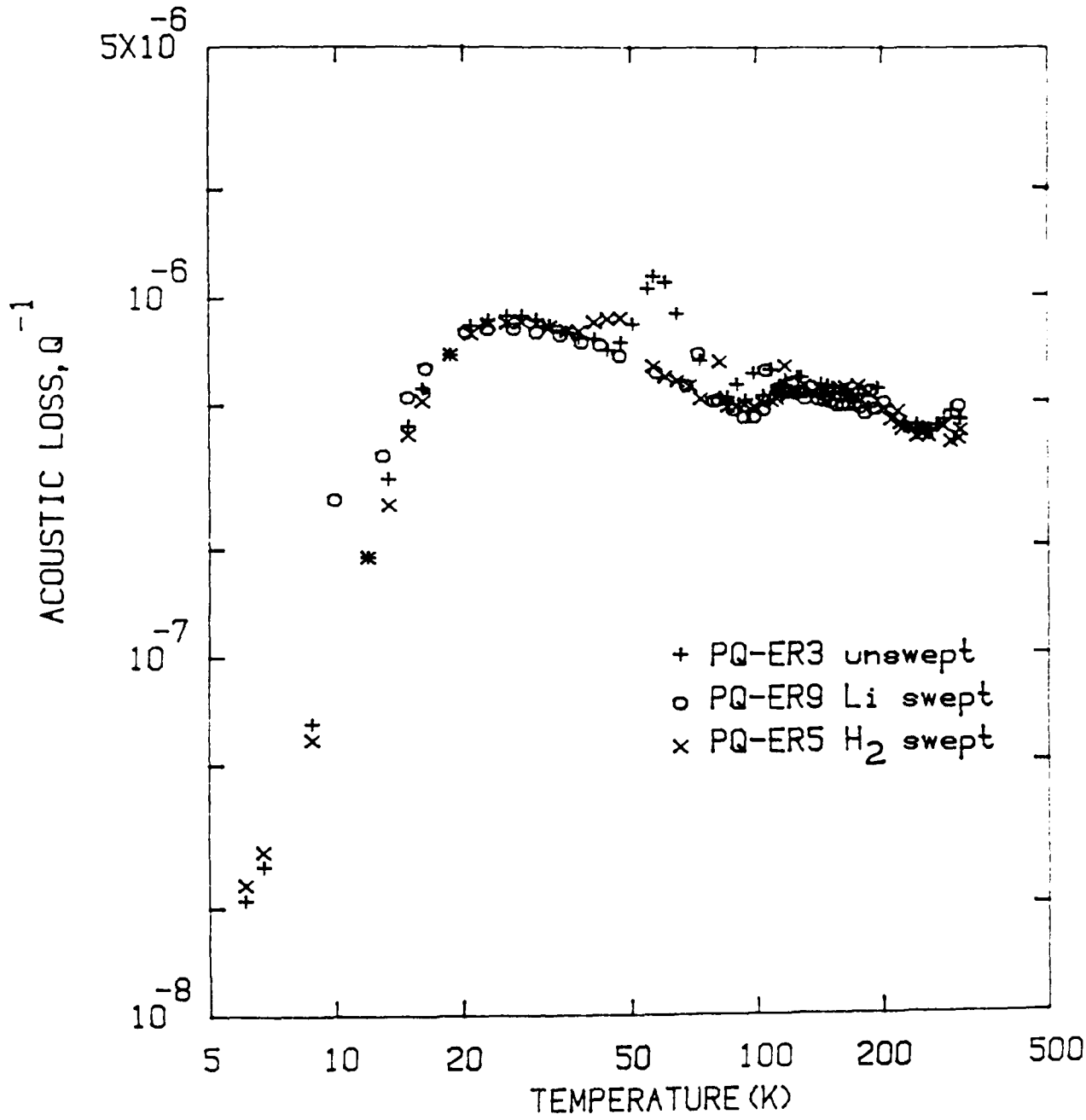

Figure 9. The acoustic loss, Q^{-1}, versus temperature spectra are shown for unswept, hydrogen, and lithium swept PQ-E series resonator blanks.

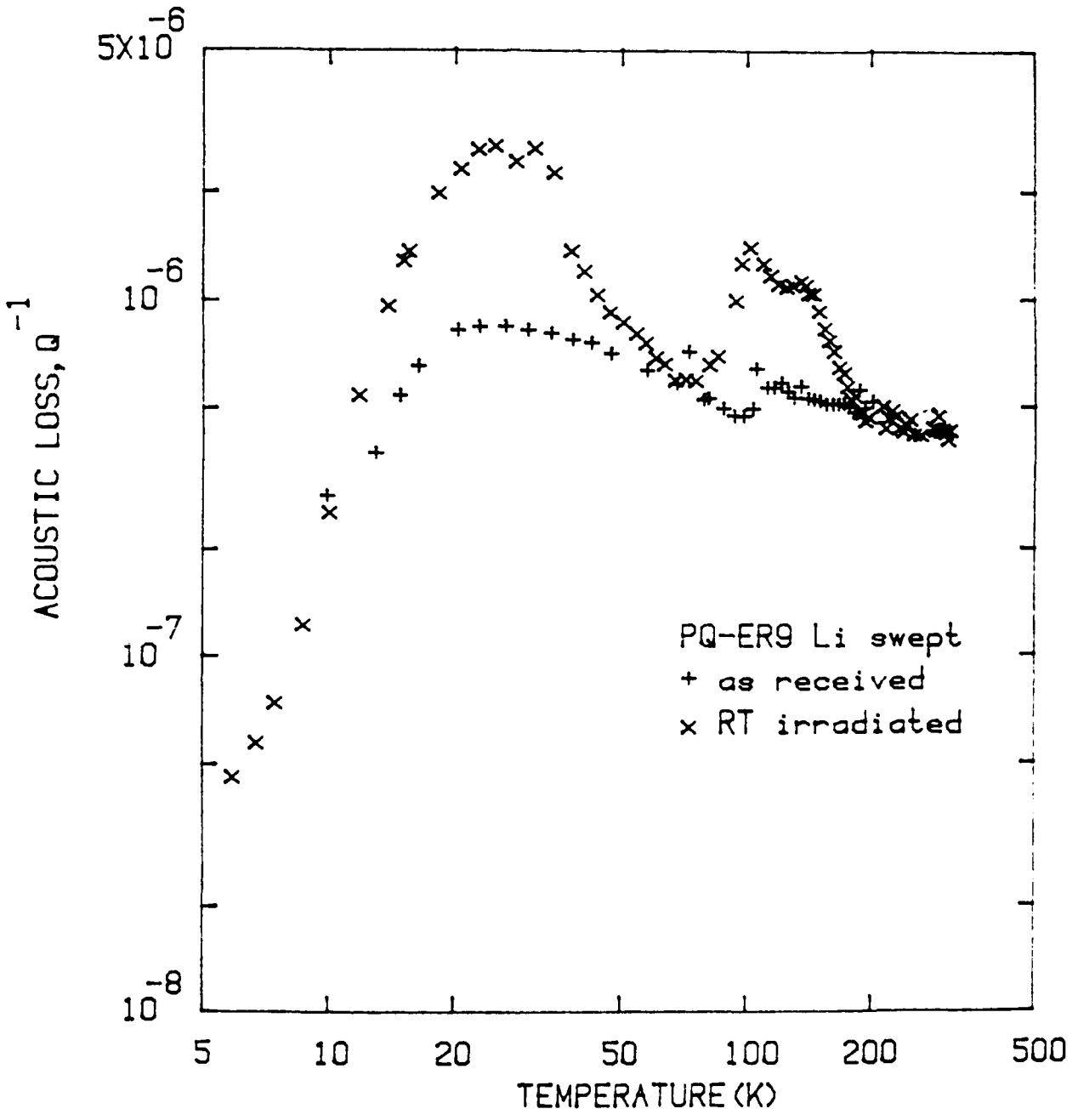

Figure 10. The acoustic loss spectrum of the lithium-swept resonator blank shows radiation-induced loss peaks at 25 K, 100 K, and 135 K. The same peaks are observed in unswept blanks. In hydrogen-swept blanks the three peaks are significantly reduced.

Defect-related acoustic loss peaks can be described by

$$\Delta Q^{-1} = D\omega\tau/(1 + \omega^2 \tau^2) \qquad (1)$$

where ΔQ^{-1} is the loss above the intrinsic background, D is the strength factor, ω is the angular frequency, and τ is the relaxation time for reorientation of the defect. The relaxation time is usually thermally activated as the defect must go over an energy barrier to reach the equivalent sites.[36] Thus,

$$\tau = \tau_o \exp(E/kT) \qquad (2)$$

where E is the barrier height and τ_o contains the number of equivalent orientations and the attack rate. We have fit Eq. 1, with the relaxation time given in Eq. 2, to the Al-Na^+ center loss peak and to the three radiation-induced peaks. For purposes of this calculation the broad loss between 125 K and 165 K is described by a single peak centered at 135 K. The calculated parameters are listed in Table IX.

Table IX. Loss Peak Parameters

T(k)	E(meV)	τ_o(sec)	Defect
54	55	2.5×10^{-13}	Al-Na^+
25	8	8.3×10^{-10}	Al-hole
100	90	1.0×10^{-12}	Al-hole
135	110	2.7×10^{-12}	Al-hole

Our activation energy and relaxation time for the Al-Na^+ center loss peak are in excellent agreement with those determined by Stevels and Volger[36] from dielectric loss measurements. Stevels and Volger have also reported a radiation-induced dielectric loss peak with E = 7.5 meV and $\tau_o = 5 \times 10^{-7}$ sec. This activation energy is in reasonable agreement with our 25 K peak, but the relaxation time is much longer. Taylor and Farnell[37] have also made dielectric loss measurements on irradiated quartz; they found a loss peak near E = 7.5 meV in agreement with Stevels and Volger and an additional peak at low temperature with E = 1.2 meV and $\tau_o = 6.2 \times 10^{-5}$ s.

The thermal anneal behavior of the Al-hole and $Al\text{-}OH^-$ centers in unswept quartz has been studied by Marks and Halliburton[22] and by Sibley et al.,[14] respectively. The Al-hole center, as observed by ESR techniques, anneals out slightly below 300°C while the $Al\text{-}OH^-$ center anneals out between 350°C and 400°C. These results strongly suggest that the alkali does not return to the aluminum site until the 350°C to 400°C range is reached. If the three radiation-induced loss peaks are due to the Al-hole center, they should show the same annealing pattern as the Al-hole center ESR spectrum. We have carried out an isochronal anneal study on the unswept blank and found that the 25 K, 100 K, and 135 K loss peaks all anneal out at 270°C, as shown in Fig. 11. Thus, all three loss peaks are most likely caused by the Al-hole center. When the anneal is continued to higher temperatures, the $Al\text{-}Na^+$ center loss peak recovers between 350°C and 400°C as shown in Fig. 11. The anneal of the $Al\text{-}OH^-$ center, as measured by infrared absorption, in a room-temperature-irradiated unswept optical sample taken from the PQ-E bar is also shown in Fig. 11. The $Al\text{-}OH^-$ strength grows slightly when the Al-hole centers decay and then goes out when the Na^+ ions return to the Al sites.

D. Conclusions

When a Premium Q resonator blank was swept with Li, the 54 K $Al\text{-}Na^+$ center peak was removed from the acoustic loss versus temperature spectrum but no new peak that could be attributed to the $Al\text{-}Li^+$ center was observed. Therefore, we conclude that the $Al\text{-}Li^+$ center shows much less coupling to the AT thickness shear mode than the $Al\text{-}Na^+$ center. Both unswept and Li-swept Premium Q blanks show

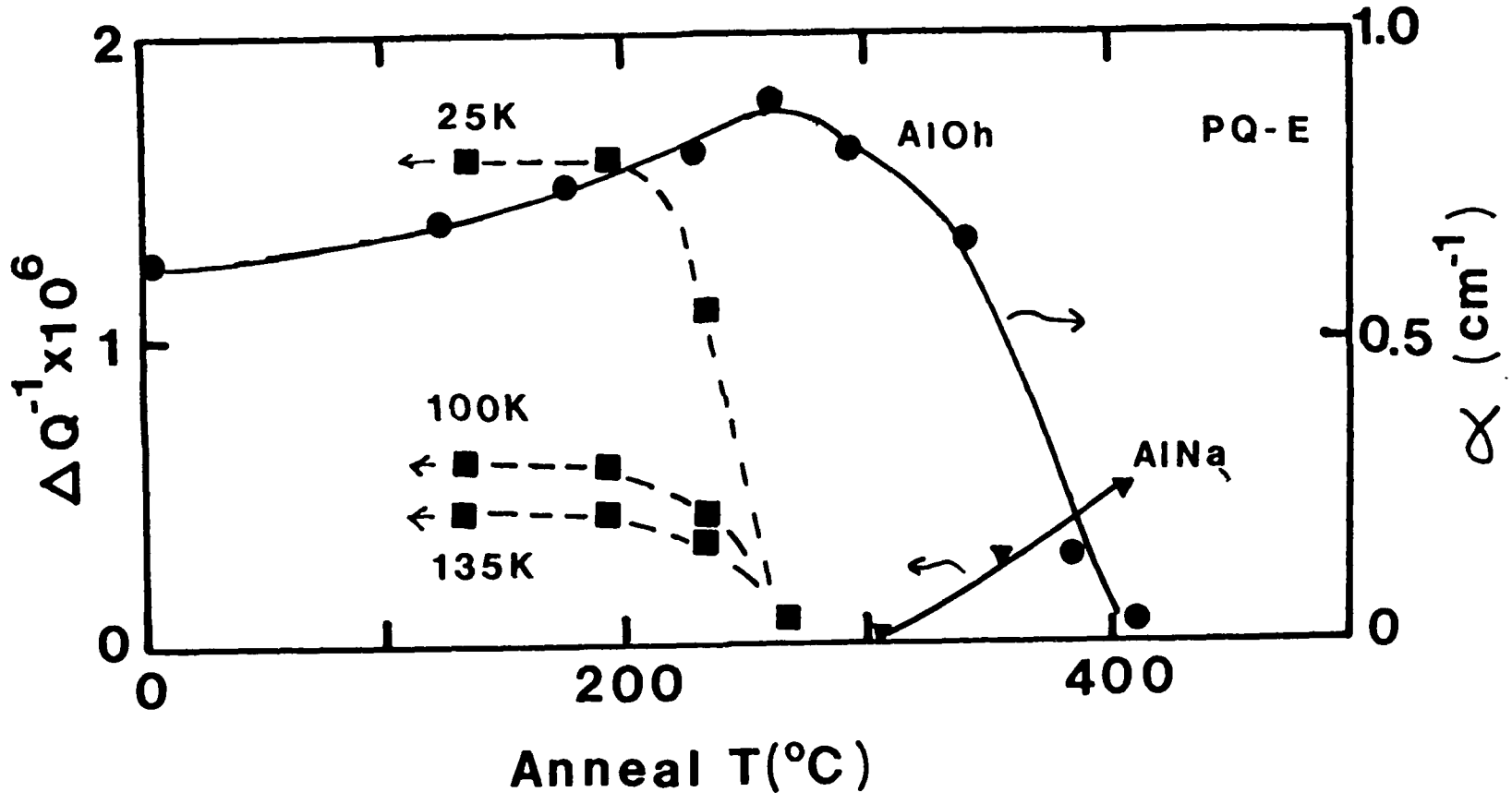

Figure 11. The 25 K, 100 K, and 135 K radiation-induced loss peaks anneal out together at the same temperature as the Al-hole center. The Al-OH^- center anneals out when the Al-Na^+ loss peak returns above 350°C.

large acoustic loss peaks at 25 K, 100 K, and 135 K when they are irradiated at room temperature. These peaks are also present in H_2- swept material, in which case they are approximately 20% of the height observed in the unswept quartz. Annealing studies show that all three of these loss peaks are due to the Al-hole center and that it anneals out at 250°-300°C. The Al-Na^+ center loss peak which is removed by a room temperature irradiation returns for annealing temperatures above 350°C. The Al-OH^- center in unswept material anneals out at that same temperature.

IV. MAGNETIC RESONANCE

A. Introduction

Electron spin resonance (ESR) studies in high-quality cultured quartz help provide information about impurity contents and defect structures. Among the first ESR results on radiation-induced defects in quartz was the report by Weeks[38] of the oxygen-vacancy-associated trapped electron center, now known as the E_1' center. Further experimental work on the E_1' center was carried out by Silsbee,[39] whereas Feigl, Fowler, and Yip[40] theoretically analyzed this center in order to provide more information on its electronic structure.

Similar oxygen-vacancy-associated trapped electron centers involving hydrogen, the E_2' and E_4' centers, have been studied.[41-43] An extensive analysis of the E_4' center[44] provided a model consisting of an H^- ion trapped in an oxygen vacancy along with an unpaired electron in an sp^3 orbital of a neighboring Si ion. The E_2' center's EPR spectrum also shows a hyperfine interaction with a single hydrogen, but no definite model for this center has been proposed.

Another major paramagnetic species found in quartz is the aluminum-associated trapped hole center (Al-hole center) first observed by Griffiths et al.[15] O'Brien[16] was able to explain the electron spin resonance data for the Al-hole center by a model having a hole trapped in a non-bonding orbital of an oxygen ion adjacent to a substitutional aluminum ion.

All quartz, both natural and synthetic, contains some aluminum as a substitutional impurity. Also present to charge compensate the $A\ell^{3+}$ which replaces a Si^{4+} are interstitial ions, usually H^+, Li^+, and Na^+. Their presence has been observed in the electron-like germanium centers in quartz studied by Anderson and Weil[45] and by Mackey.[17] Mackey[17] and Mackey et al.[18] have also studied aluminum-associated trapped hole centers involving an interstitial impurity ion. These latter centers are designated by $[A\ell_e+/M^+]^+$ where M^+ represents an interstitial H^+, Li^+, or Na^+ charge compensator. Such centers are created by ionizing radiation below room temperature (usually at 77 K) and are only stable at these lower temperatures.

Quartz has large c-axis channels along which interstitial ions can move. Kats[10] applied an electric field parallel to the c-axis and was able to "sweep" in or out hydrogen and alkali ions for samples temperatures in the 400°C to 550°C range. Sweeping is very useful in providing a single type of charge compensator and helps in defect identification studies. Sweeping in hydrogen to replace alkalis has been reported[46] to increase the radiation hardness of quartz resonators.

Markes and Halliburton[22] found, in high quality quartz grown using sodium carbonate as the mineralizer, the majority of aluminum impurity ions are charge-compensated by neighboring interstitial Na^+ ions. They found that electron irradiation above 200 K removed the Na^+ interstitials from the $A\ell$ sites and either Al-hole or $A\ell$-OH^- centers were created. A short re-irradiation at 77 K would convert all the $A\ell$ sites to Al-hole centers indicating that at 77 K the interstitial hydrogen ions have radiation-induced mobility. Heating the samples above 600 K causes the alkali ions to return to the $A\ell$ sites and the sample is restored to its pre-irradiated state. These results provide a procedure for testing the effectiveness of the sweeping process in removing interstitial alkali ions from the quartz samples.[22]

B. Experimental Procedure

High quality synthetic quartz crystals were obtained from Sawyer Research Products[47] and Toyo Communications Equipment Company.[48] The lumbered bars of pure Z-growth material were cut with a diamond saw into small samples (3 x 8 x 12 mm^3) for use in the ESR studies. The Sawyer samples were Premium Q (PQ) grade quartz from unswept and swept (by Sawyer) bars. The Toyo quartz samples were from a Toyo Supreme Q (SQ) bar.

All irradiations were performed using 1.7 MeV electrons from a van de Graaff accelerator. The 77 K irradiations were done with the sample immersed in liquid nitrogen, and the 0°C irradiations with the sample immersed in an ice bath. The variable temperature irradiations were performed using a nitrogen gas flow system where nitrogen gas of the desired temperature flows by the sample while it is being irradiated. All of the ESR spectra shown in Section IV were taken at room temperature.

The ESR spectrometer used was a Varian 4500 using 100 kHz modulation and operating at 9.23 GHz. The magnet was a Varian 12 inch Fieldial-regulated and a Narda N6244S-37 microwave amplifier was added to the bridge increasing the sensitivity especially at lower microwave power. A Varian Variable Temperature Accessory V-4557 using a nitrogen gas flow permitted thermal anneal studies up to 200°C. A Varian E-500 digital gaussmeter and an HP 5340A microwave frequency counter were used to measure g values and magnetic field splittings.

C. Results

When samples of high quality quartz (PQ and SQ) are electron irradiated at 0°C (ice bath), the ESR spectrum (taken at room temperature) shown in Fig. 12 is observed when the magnetic field is parallel to the c-axis. Since the ESR linewidths are extremely narrow (< 0.05 G) the phase of the 100 kHz modulation unit was adjusted to prevent modulation "sidebands" from appearing and giving distorted ESR lineshapes. All ESR spectra were recorded with the phase adjusted in this manner.

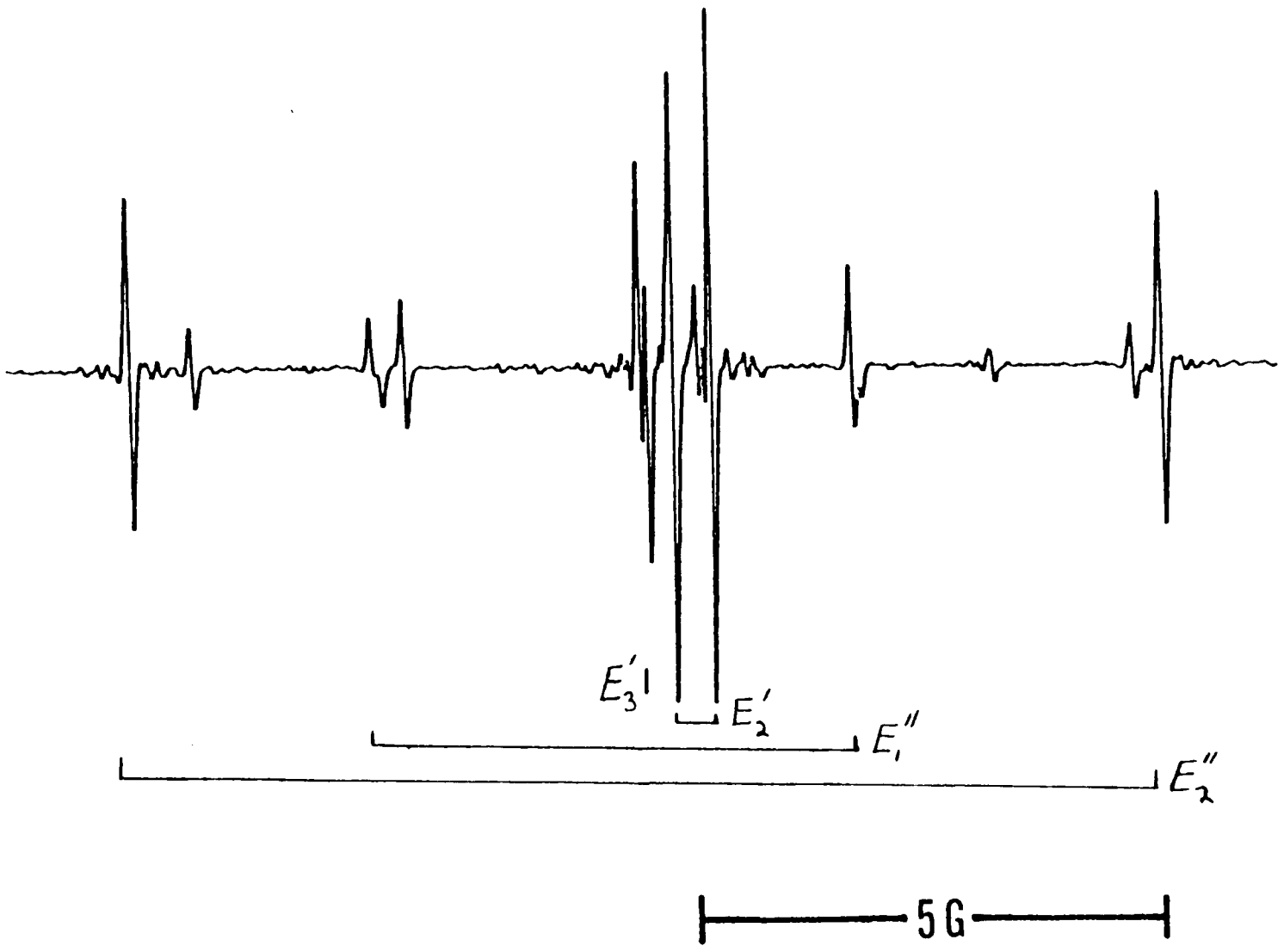

Figure 12. ESR spectrum of Premium Q quartz taken at room temperature following an electron irradiation at 0°C.

Figure 12 shows ESR lines due to E_2' centers. In addition, three other ESR doublets labeled E_3', E_1'', and E_2'' are also observed.

If the sample is given a short 77 K electron irradiation, the ESR spectrum shown in Fig. 13 is obtained when the magnetic field is parallel to the c-axis. The E_2' and E_3' signals are gone but the E_1'', E_2'', and a new doublet labeled E_3'' are very prominent. The c-axis g-values and magnetic field separations of these doublets are given in Table X.

The small doublet labeled E_3' and the center labeled E_2'' decay slowly at room temperature and disappear in about 6 hours. The E_3' center appears to be an $S = \frac{1}{2}$ center interacting weakly with a 100% abundant $I = \frac{1}{2}$ nucleus (probably hydrogen). The other doublets labeled E_1'', E_2'', and E_3'' exhibited a large anisotropy in magnetic field splittings characteristic of S = 1 spin systems. Weeks and Abraham[49,50] reported seeing S = 1 centers in 1.5 MeV electron-irradiated quartz which was ^{60}Co γ-irradiated at 77 K. The S = 1 centers we have observed appear to be the same as Weeks observed and we have given them E'' labels, indicating two unpaired spins forming an S = 1 center. Weeks and Abraham took only a rough angular variation of the most intense S = 1 center and did not determine accurate spin-Hamiltonian parameters. We have made an accurate angular variation of the ESR spectrum for the E_1'' center which is shown in Fig. 14.

The isothermal pluse anneal results shown in Fig. 15 for the E'' centers describe the thermal stability of these centers for 5 minute anneals at each temperature. The ESR spectra were recorded at 0°C after each anneal. The E_2'' centers anneal out at 40°C while the E_1'' and E_3'' centers are more stable and are gone by 90°C.

It was found that the E'' centers could be produced in all unswept quartz samples by a short 77 K irradiation provided the samples had previously received an electron irradiation at room temperature. A variable temperature electron irradiation of an as-grown PQ quartz sample was performed where each irradiation

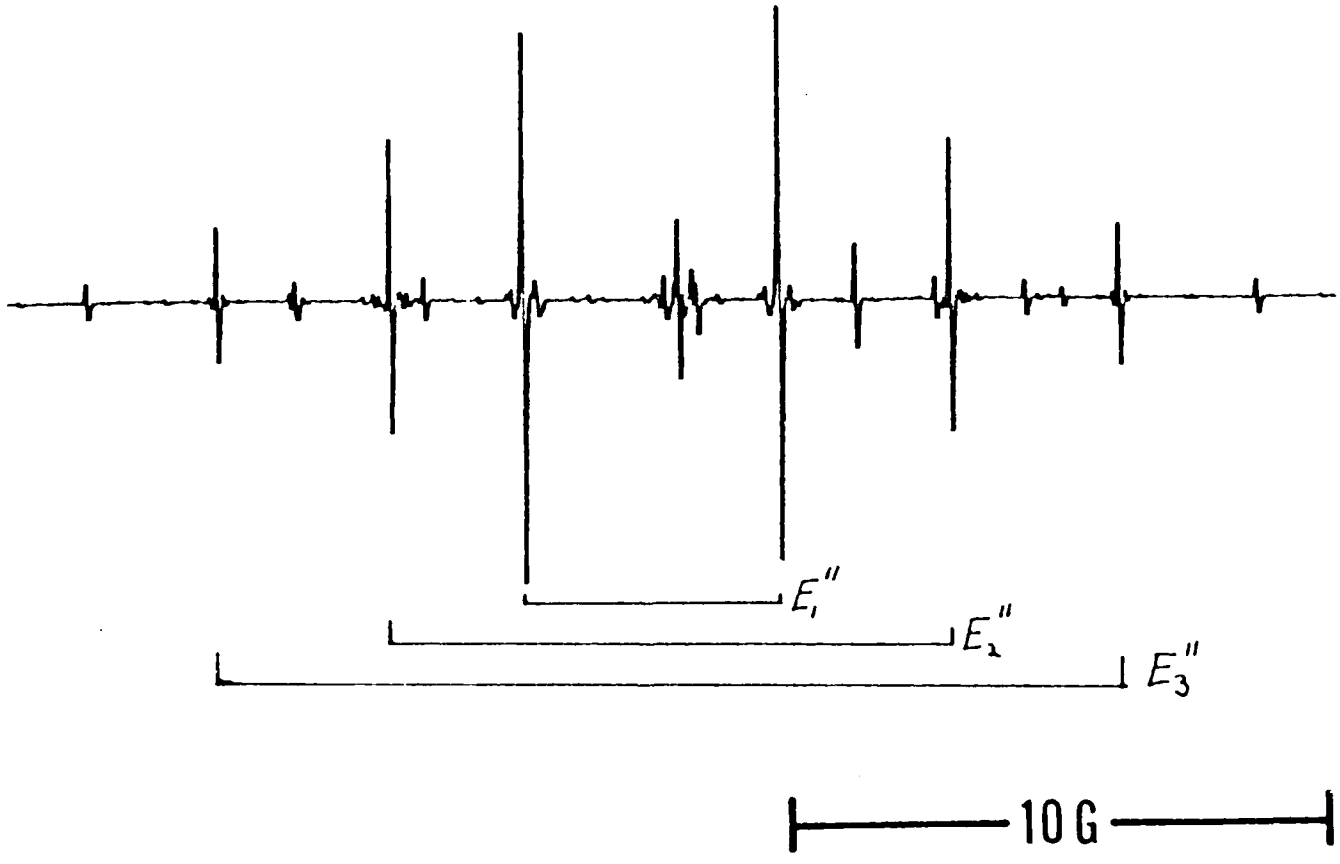

Figure 13. ESR spectrum of Premium Q quartz taken at room temperature following an electron irradiation at 77 K. The sample had been previously irradiated at room temperature.

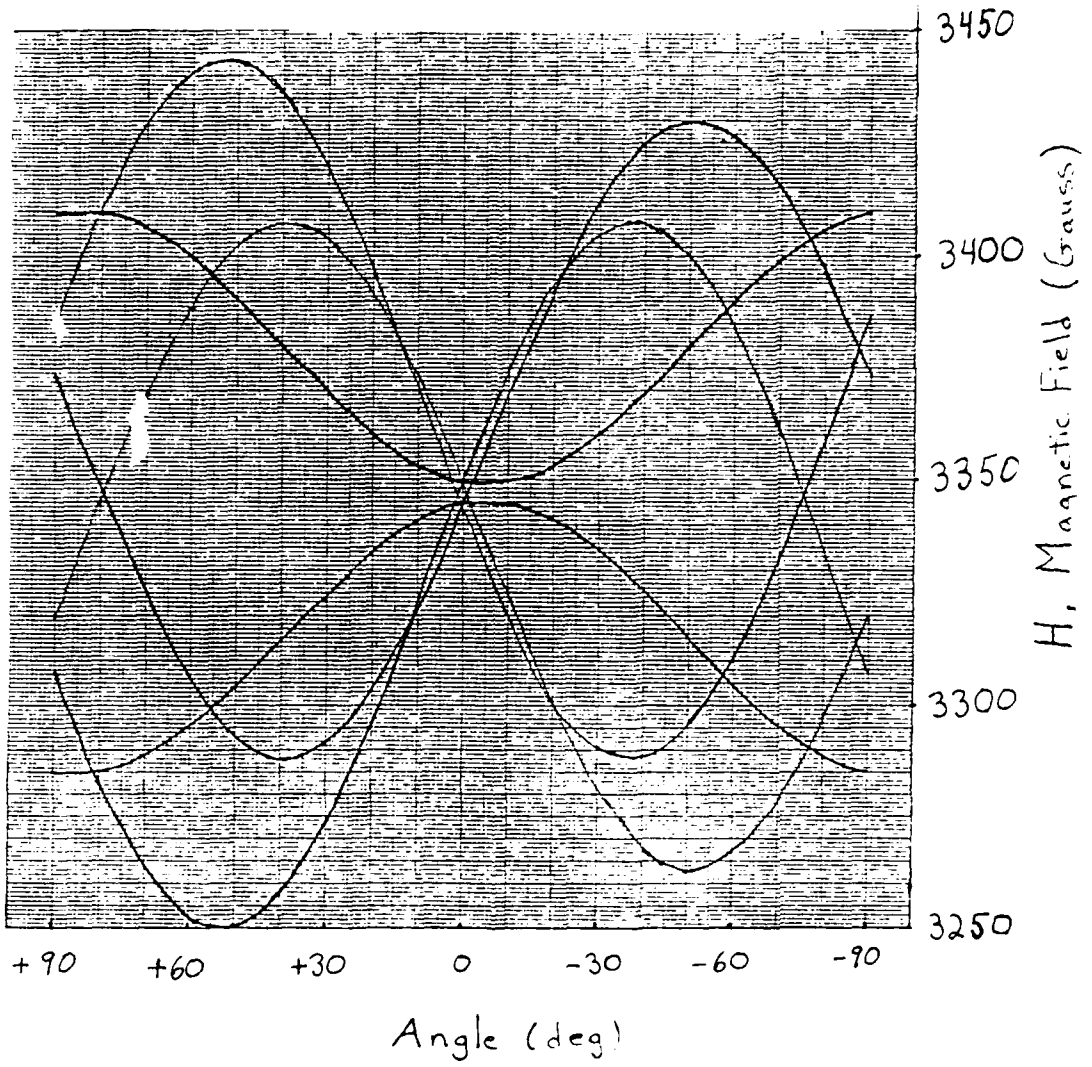

Figure 14. Angular variation of the ESR spectrum for the E_1'' center.

Figure 15. Isochronal anneal results for the E" centers.

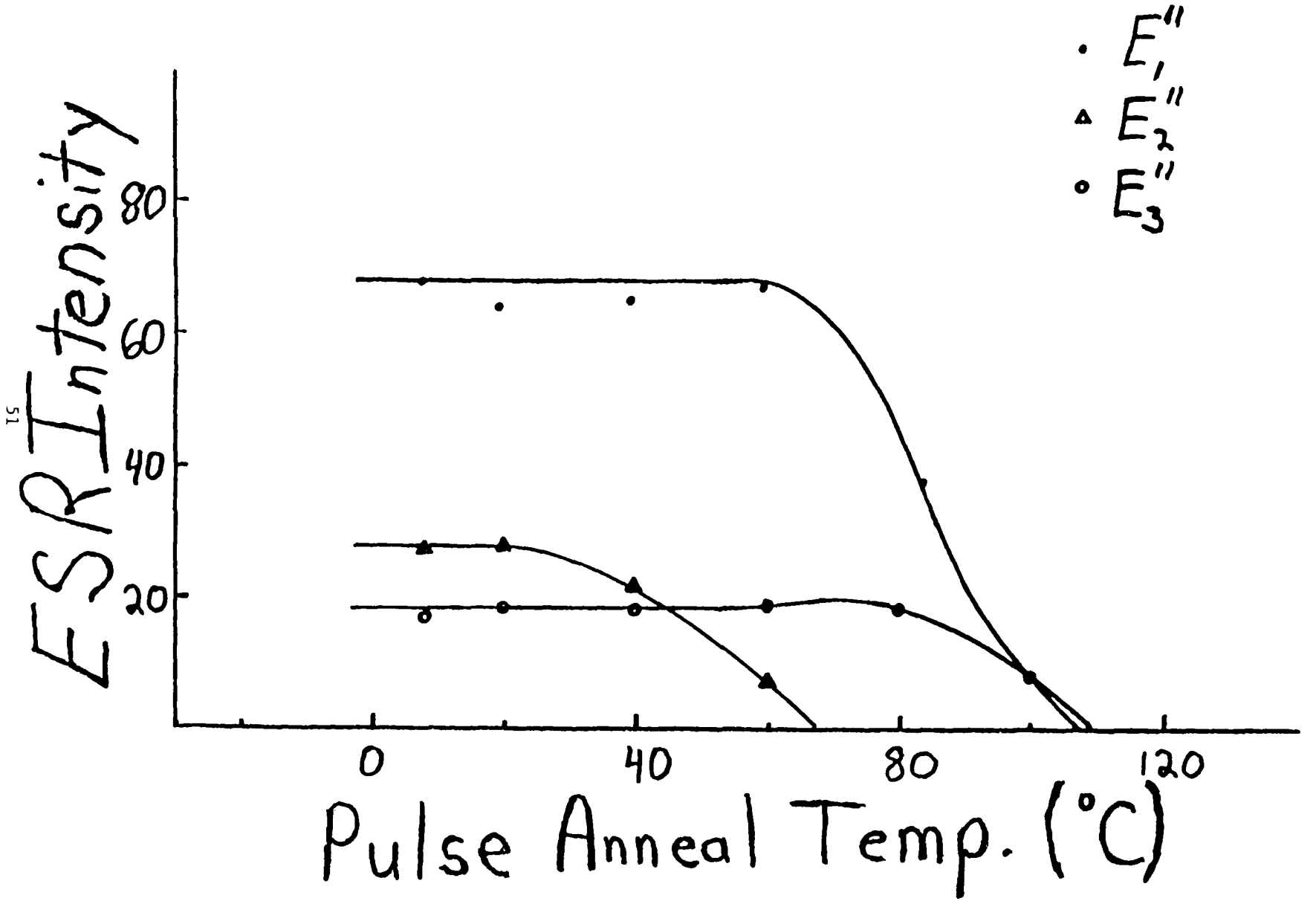

TABLE X. The c-axis g values and line separations for paramagnetic defects produced by electron irradiation of Sawyer PQ and Toyo SQ quartz. The E_2' and E_4' centers have splittings due to a hyperfine interaction with a proton, and this is probably the cause of the small splitting observed for the E_3' center. The E'' centers have c-axis splittings due to their S = 1 defect configuration.

Center	g_c	ΔH_c(G)
E_2'	2.0005	0.4
E_3'	2.0010	0.1
E_4'	2.0011	~5 (4 lines)
E_1''	2.0011	5.0
E_2''	2.0010	11.0
E_3''	2.0010	17.8

was followed by a short 77 K irradiation (necessary to populate the E'' centers). Figure 16 shows the results which indicate that the 77 K irradiation will not produce the E'' centers unless the sample has received an electron irradiation above 200 K. Markes and Halliburton[15] have found in ESR studies of the $[Al_e+]^o$ center in quartz that this is the temperature at which Na^+ interstitial ions become mobile under electron irradiation. The removal of the intersititial will leave substitutional Al^{3+} ions, allowing an enhanced Al-hole population to be created by a subsequent 77 K irradiation. For E'' centers it is therefore necessary to perform an irradiation above 200 K before a 77 K irradiation, in order for them to be observed using ESR. In Sawyer-swept samples where the alkali ions have been replaced by hydrogen, Markes and Halliburton found no enhancement in the number of Al-hole centers following the above 200 K irradiation. We have observed only very small numbers of E'' centers in Sawyer-swept PQ quartz. This indicates that the alkalis (Na^+, Li^+) must be present in the quartz samples and removed from the Al^{3+} substitutional ions (by above 200 K irradiation) in order for the E'' centers to appear.

The growth of E'' centers with room-temperature-irradiation time where each room-temperature electron irradiation was followed by a short 2 minute irradiation at 77 K is illustrated in Fig. 17. This shows that the process for moving the alkali ions away from the aluminum impurity sites occurs fairly slowly. The approximate dose on the sample after 20 minutes of irradiation time is 2×10^{15} e^-/cm^2.

Although the magnetic resonance signals for the E'' centers were observed to thermally anneal out by 100°C, they could be recreated by a short 77 K irradiation. A high temperature thermal anneal was performed to see if there was a point where the E'' centers could not be recreated by the 77 K irradiation. Figure 18 shows the high temperature anneal results for a PQ quartz sample where each anneal was followed by a short 77 K electron irradiation. After an anneal temperature of 600 K,

Figure 16. Production of F" centers as a function of irradiation temperatures in a Premium Q sample which had not been previously irradiated.

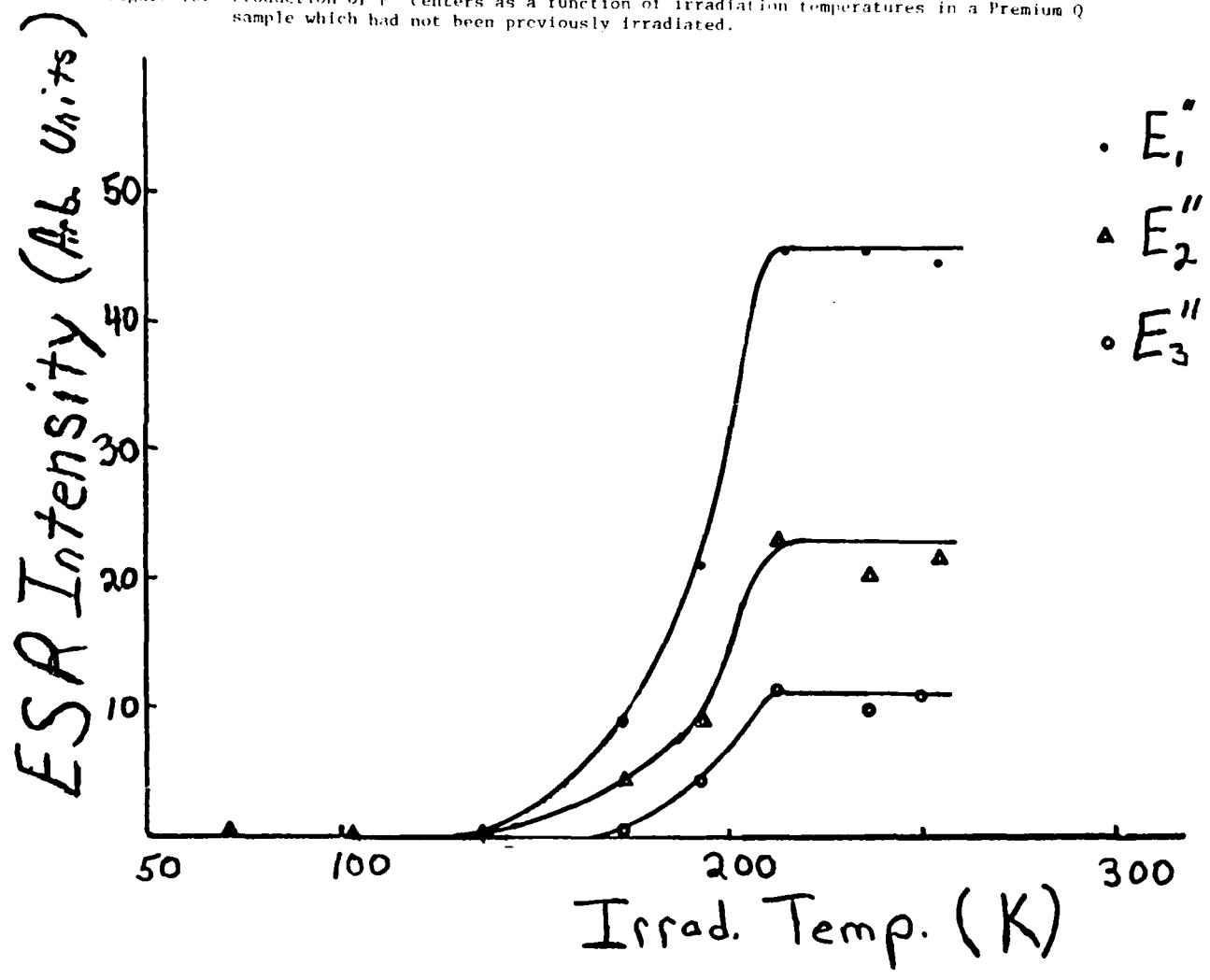

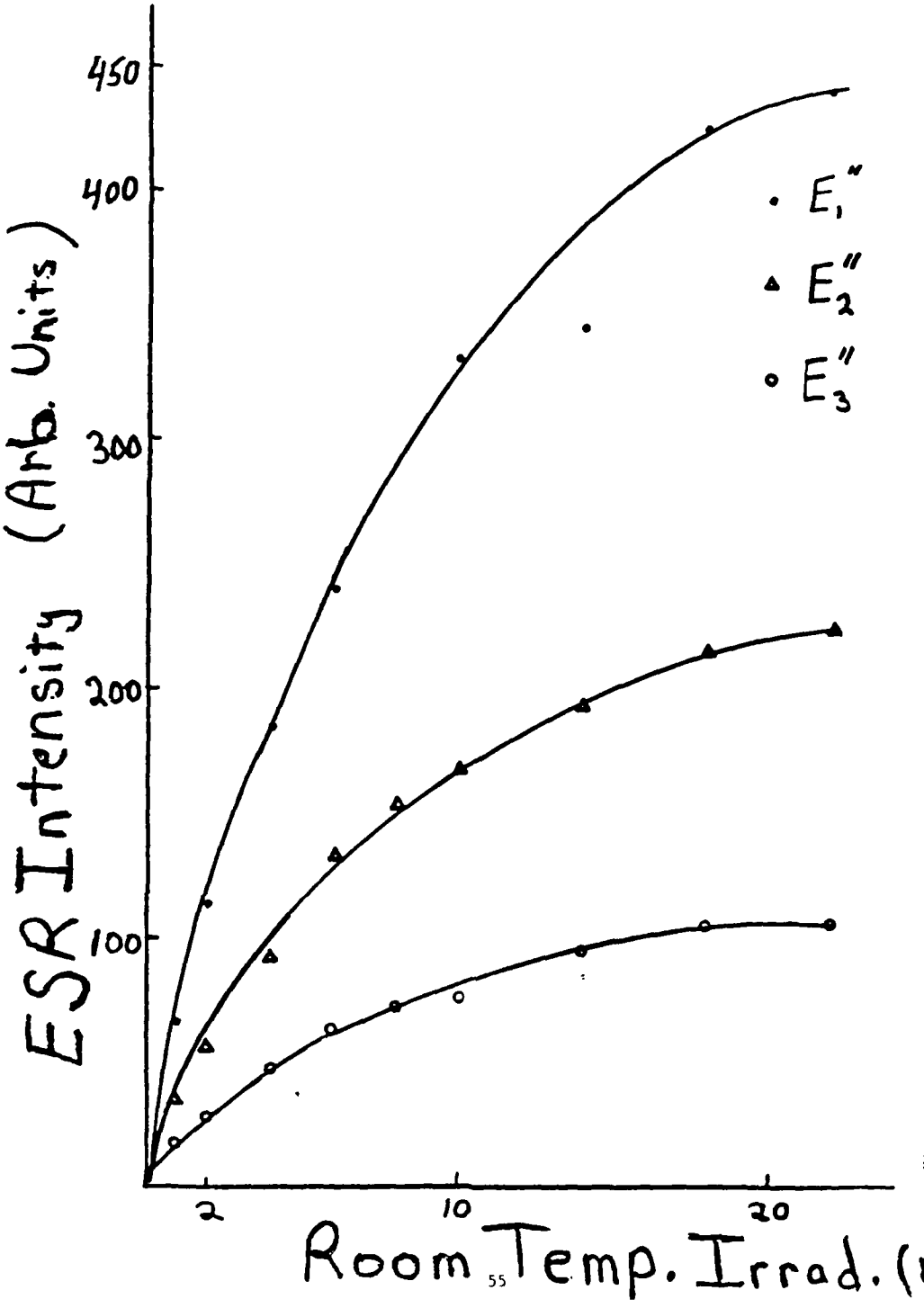

Figure 17. Growth of F'' centers as a function of room temperature irradiation.

Figure 18. High temperature anneal and recreation of E'' centers.

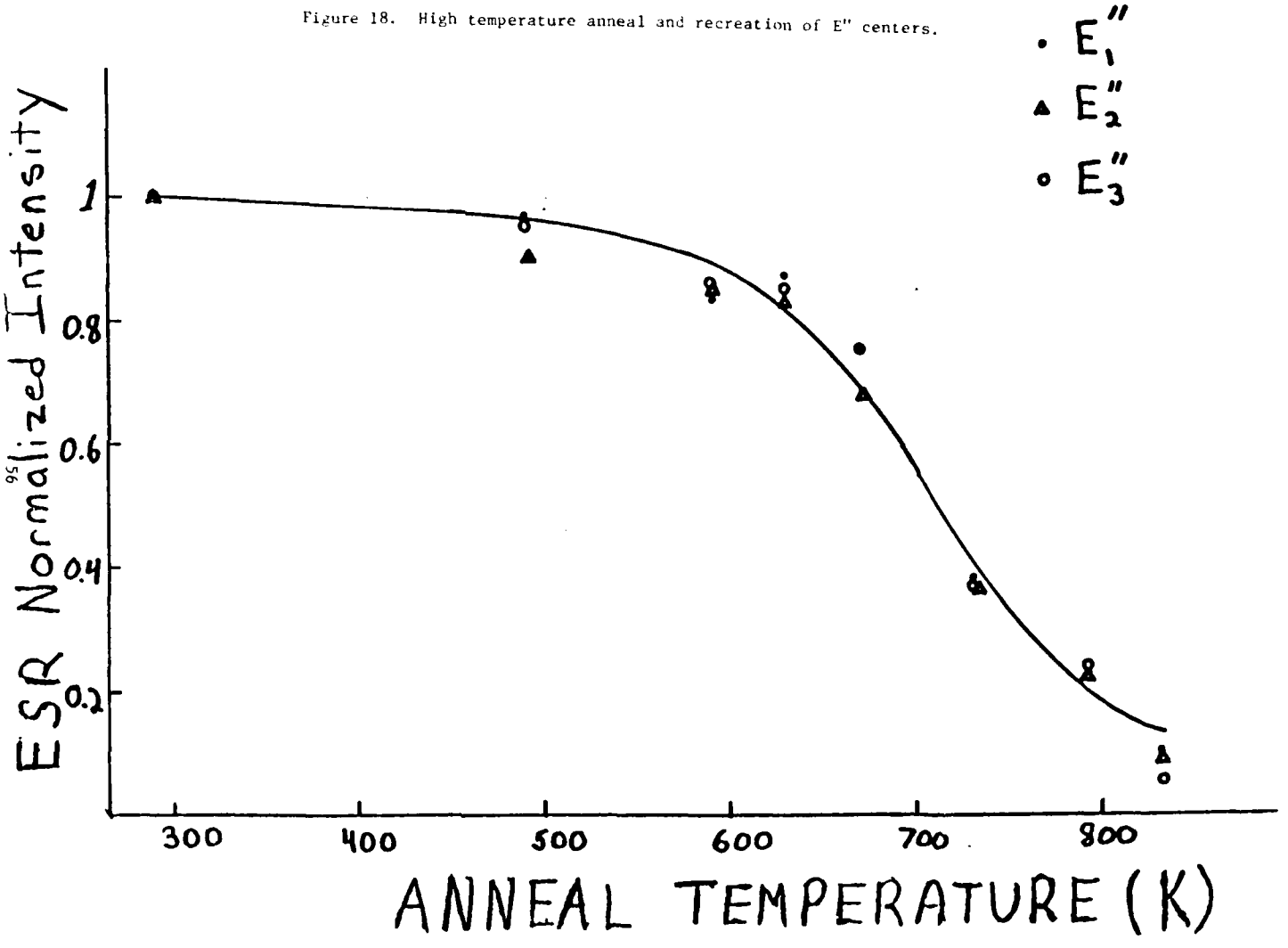

the number of E'' centers formed by the 77K irradiation is seen to decrease. This is the same temperature range in which Markes and Halliburton[22] found the Al-hole center production to decrease. This decrease was attributed to the return of the alkali ions to the aluminum impurity sites. Thus, a high-temperature anneal will return the quartz sample to its as-grown state and the E'' centers will not be created by only a 77 K irradiation.

D. Discussion

The highly anisotropic angular variation of the ESR spectrum for the E'' centers indicates that they are S = 1 centers. We have also detected for the E_1'' center the $\Delta M_S = 2$ "half-field" transition confirming its S = 1 nature. Using the following spin Hamiltonian for S = 1

$$\mathcal{H} = \beta\vec{H}\cdot\vec{g}\cdot\vec{S} + \vec{S}\cdot\vec{D}\cdot\vec{S}$$

and the angular variation data for the E_1'' centers, the g and D tensor principal values and directions given in Table XI were calculated by a least squares fitting procedure. It is hoped that interpretation of these parameters will lead to a definitive model for the E'' centers.

The correlation of the ESR results for the E'' centers with the previous results for the Al-hole center will help us determine the role the E'' centers play in the overall response of high quality quartz to radiation. The fact that the E'' centers are not seen in Sawyer-swept samples of PQ quartz indicates that the alkalis play some role in the stabilization of the E'' defects. Also the alkalis must be moved away from the Al impurity sites before the E'' centers are observed. Hopefully, continued study of the E'' centers as well as the Al-hole and single electron centers (E' centers) through ESR and other techniques will give a more complete understanding of the defect structure of high quality quartz crystals.

TABLE XI. Principle values and angles of the g and D tensors for the E_1'' center in quartz. (D in MHz.)

$g_x = 2.0004$	$\theta = 33.1$	$\phi = 54.1$
$g_y = 2.0006$	$\theta = 91.8$	$\phi = -33.1$
$g_z = 2.0014$	$\theta = 57.0$	$\phi = 58.0$
$D_x = 110.6$	$\theta = 34.5$	$\phi = 67.0$
$D_y = 117.2$	$\theta = 85.1$	$\phi = -30.2$
$D_z = -227.7$	$\theta = 56.0$	$\phi = 56.5$

V. THERMOLUMINESCENCE

A. Introduction

Since many applications of SiO_2 require the special properties of this high-purity material in its crystalline form, quartz, there is a continuing need for developing reliable procedures to evaluate the quality of crystals in a nondestructive manner. One purpose of this report is to present evidence that the technique of thermally stimulated luminescence, TSL, can be used as a means of determining the quality of high-purity quartz specimens and that it shows promise of being capable of characterizing certain defects present by type and concentration.

Direct monitoring of the $Al\text{-}M^+$ centers, where M^+ represents an alkali ion, presents the greatest experimental difficulty since it requires precise fabrication and mounting of resonators for acoustic loss measurements in a variable temperature helium Dewar.[28] Recently, during a study aimed at providing a definitive picture of the role of aluminum in the radiation response of quartz, Halliburton et al.[52] developed another evaluation method by calculating absolute concentrations of $Al\text{-}OH^-$ and Al-hole centers for irradiations at 77 K, 300 K, and then a reirradiation at 77 K. (See Section II of this report.) In this work the assumption was made that the sum of the concentrations of all three types of centers remained constant and that different treatments simply changed one type of compensator for another. In this way the presence of $Al\text{-}M^+$ centers could be inferred from the absence of $Al\text{-}OH^-$ and Al-hole centers. As shown in this work, TSL holds high promise of providing comparable $Al\text{-}M^+$ center information from one simple experiment.

An effective method of reducing the concentration of $Al\text{-}M^+$ centers is the electrodiffusion ("sweeping") process initially developed by King[4] and used since that time by many investigators as a technique for changing the relative concentrations of charge-compensating hydrogen and alkali ions in defect identification studies.

Particularly pertinent is the report[7] that sweeping prior to fabrication increases the radiation hardness of quartz crystals used in precision oscillators. The advantage of the development of a simple screening procedure to measure the completeness of a sweeping process is evident.

TSL in quartz has been studied by many investigators. Numbered among them, for example, are Yokota,[53] Arnold,[54] Batrak,[55] McMorris[56] and Durrani,[57] who have looked at glow peaks above room temperature in a wide variety of natural and/or synthetic crystals. The results of these studies proved to be very sample-dependent and attempts to relate individual glow peaks to specific defect centers and changes in charge state have met with, at best, limited success. Low temperature TSL has received less attention. Medlin[58] studied both natural and synthetic specimens below and above room temperature and for single crystal material observed strong glow peaks at 190 K and 210 K as well as four minor peaks between 90 K and 150 K. He attempted a systematic survey of the effect of adding different cation impurities during the crystallization process but concluded that of the more than twenty tried, only Ti^{4+} affected the glow curves of the synthetic samples. The addition of this impurity gave rise to an intense glow peak at 165 K. The emission spectrum for the 165 K glow peak consisted of several closely spaced bands in the 400-700 nm region. Other glow peaks showed an emission maximum near 380 nm. Schlesinger,[59] working mainly with Ge-doped crystals, observed low temperature glow maxima from 190 K to 300 K and used a re-excitation technique to conclude that the main glow peaks in this material were due to thermally-released electrons. The 257 K peak, however, was assigned to thermally-released holes. Levy and collaborators using gamma-irradiated natural and synthetic crystals[60] found all significant TSL output was contained in the region between 150 K and 220 K with at least four resolvable glow peaks corresponding to different charge traps. The origins of the traps and whether they trapped holes or electrons was not determined. The emission spectrum at 180 K could be accurately described by a single Gaussian band

with maximum at 380 nm and a half-width of 0.82 eV. The current work on extremely high purity synthetic quartz at Oklahoma State University[14,22,27,28,52] has shown that under irradiation, hydrogen ions are mobile at all temperatures while interstitial alkali-metal ions only become mobile above 200 K. The TSL investigation reported here is confined to the range below room temperature where radiation-induced mobility effects are prominent.

B. Experimental Procedure

Samples were taken from single crystal ingots of both Electronic Grade and Premium Q material purchased from Sawyer Research Products, Eastlake, Ohio and from a Supreme Q bar obtained from Toyo Communications Equipment Company, Kawasaki, Japan. Only Z-growth material was investigated. Since other experimenters have made use of specimens from the same bars, impurity analyses, autoclave, and electrodiffusion ("sweeping") information are available in their papers.[22,52] Although certain sweeping techniques have been developed locally, all swept samples studied in this work were purchased as such from Sawyer where they had been swept in air. Data in the last three columns of Table XII are taken from the work of Halliburton *et al.*[52] and show the $Al\text{-}M^{+}$, $[Al_e+]^{o}$ (aluminum-hole), and the $Al\text{-}OH^{-}$ concentrations deduced for samples taken from the same ingots as those used in the TSL experiments. It should be noted that the impurity concentrations in a single ingot can vary considerably, as Lipson *et al.*[12] have shown. This suggests that some care should be taken in assuming that the calculated concentrations are absolutely characteristic of the whole bar.

Samples were cut in the form of plates approximately 15 x 13 x 3 mm^3 perpendicular to the c-axis of the crystal. They were then mounted on the copper cold finger of a cryostat originally designed for low temperature optical absorption studies. A rectangular hole of 12 x 6 mm^2 in the cold finger and a matching hole in a second copper plate placed on the other side of the sample and attached to the

TABLE XII. Region III TSL peak intensities and concentrations of aluminum-associated defects for several quartz specimens treated as noted.

Specimen bar and treatment	TSL (arbitrary units)	$Al\text{-}M^+$ ($10^{16}cm^{-3}$)	$[Al_{e^+}]^o$ ($10^{16}cm^{-3}$)	$Al\text{-}OH^-$ ($10^{16}cm^{-3}$)
P_1-L (unswept)				
1st low temperature irradiation[a]	33.3	40.2[b]	0.2[b]	0[b]
300 K irradiation	...	0	15.2	13.8
2nd low temperature irradiation	0	0	40.4	0
P_1-D (swept)				
1st low temperature irradiation	0	0	15.1	0
300 K irradiation	...	0	1.0	9.2
2nd low temperature irradiation	0	0	14.6	0
P_1-A (unswept)				
1st low temperature irradiation	0.9	3.9	0	0
300 K irradiation	...	0	0.4	2.8
2nd low temperature irradiation	0	0	3.9	0
SQ-A (unswept)				
1st low temperature irradiation	17.9	32.3	0.6	0
300 K irradiation	...	0	22.8	14.8
2nd low temperature irradiation	0	0	28.4	4.5

[a] Low temperature irradiations done at 77 K for Section II and at 95 K for study reported here.

[b] Numerical values in these columns taken from Section II.

cold finger for temperature uniformity allowed the quartz specimen to be irradiated from either side and to be observed simultaneously from both sides while being warmed. Samples were irradiated at 95 K through a 0.005-inch-thick aluminum window with 1.5-MeV electrons from a Van de Graaff generator operating at a beam current of 10 μA for a total time of five minutes. Direct calibration using a glass dosimeter indicated specimens were typically irradiated to a dose of the order of one Mrad by this procedure. After irradiation, the cryostat was placed in front of an optical detection system consisting of a 0.5-meter Bausch and Lomb monochromator with an EMI 6256 photomultiplier tube connected to appropriate electronics for the determination of the spectral distribution of the TSL. The wavelength range of 200 nm to 700 nm could be scanned in 2.5 minutes. At the same time, total glow curves were observed from the opposite face of the crystal using an EMI 9558Q photomultiplier tube. A heating rate of about 11 K/min was used. Photomultiplier outputs were plotted versus wavelength and thermocouple voltage, respectively, on two Houston Instrument X-Y recorders. Comparisons of the two traces at equivalent time points and monochromator scans in both wavelength directions over the glow peak regions were used to compensate for the changes in glow peak intensity during single spectral analysis wavelength scans.

In order to gain better insight into the origin of the TSL, changes associated with a series of irradiations at different temperatures were also studied. The results thus obtained were compared with those of other local experiments[52] in which infrared, ESR, and Q properties were evaluated after similar multiple treatments. For this work the specimens were initially irradiated at 95 K with 1.5-MeV electrons as described above. Although limitations imposed by the construction of the cryostat precluded 77 K irradiations for direct comparison purposes, other evidence indicates that very little annealing of defects occurs between 77 K and 95 K.[22,27,52] After a TSL run to 300 K, the samples remained in the cryostat and were irradiated at 300 K -- or at some other specific temperature above 95 K -- for another total of 5 minutes.

They were then recooled to 95 K and reirradiated. Following multiple irradiations which produced a change in the TSL as described below, the specimen could essentially be returned to its initial condition by a 750 K anneal for ten minutes. This effect had been observed previously[14,22] through other measurement techniques.

C. Experimental Results

Figure 19 compares the TSL data for an Electronic Grade (EG-E10) and a Premium Q (PQ-A10) specimen after a 95 K irradiation. Neither of these samples had been swept. As might have been anticipated, Premium Q specimens (with an exception to be noted later) showed generally reduced TSL output. The glow peaks clearly fall into three temperature regions: Region I (115-145 K), Region II (145-185 K) and Region III (185-270 K). The general pattern of the data in regions I and III was reasonably consistent for all the unswept samples studied but both the size and number of distinguishable glow peaks in Region II were considerably more sample-dependent.

Samples which had been swept show marked differences from unswept samples as indicated in Fig. 20. Here it can be seen that for swept samples there is no emission in Region III and the emission in Region II is significantly less. The peak intensity of Region I was found to be somewhat dependent on the length of time between the irradiation and the initiation of the TSL run. It was also observed that when the initial irradiation temperatures were above 100 K, this peak was greatly reduced or missing from the glow curve.

Because total TSL output of all measured specimens was low, the simpler glow peak structure in Regions I and III yielded the most definitive spectral distribution data. In both cases the spectral peaks were broad and relatively featureless. Region I light showed a maximum around 450 nm with a half-width of about 0.5 eV. Comparable figures for Region III were 380 nm and 0.75 eV. Region II evaluations were complicated by the presence of as many as five overlapping, resolvable total

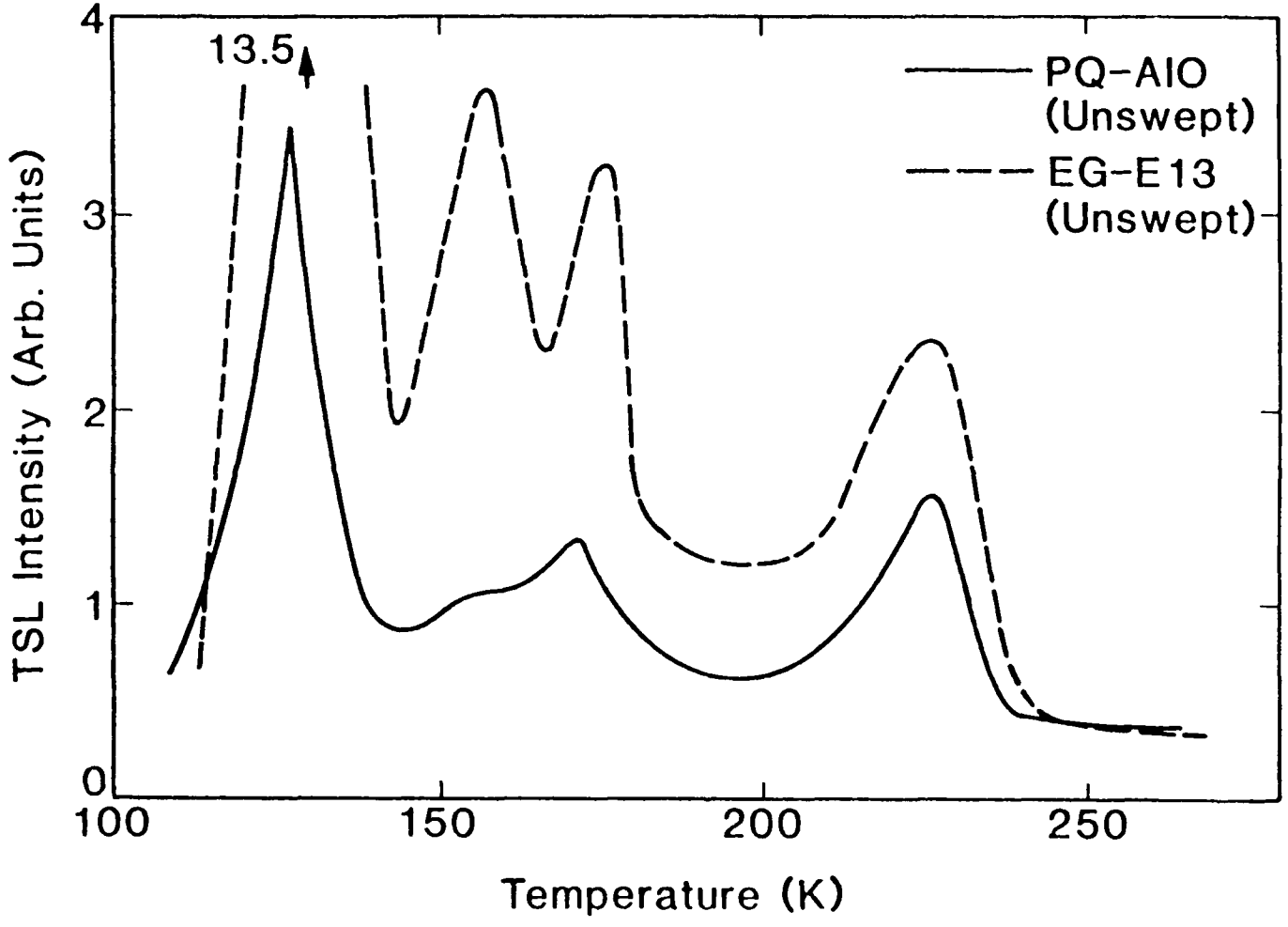

Figure 19. Comparison of TSL intensities vs temperature for unswept Premium Q (PQ-A10) and Electronic Grade (EG-E13) specimens. Irradiation temperature was 95 K.

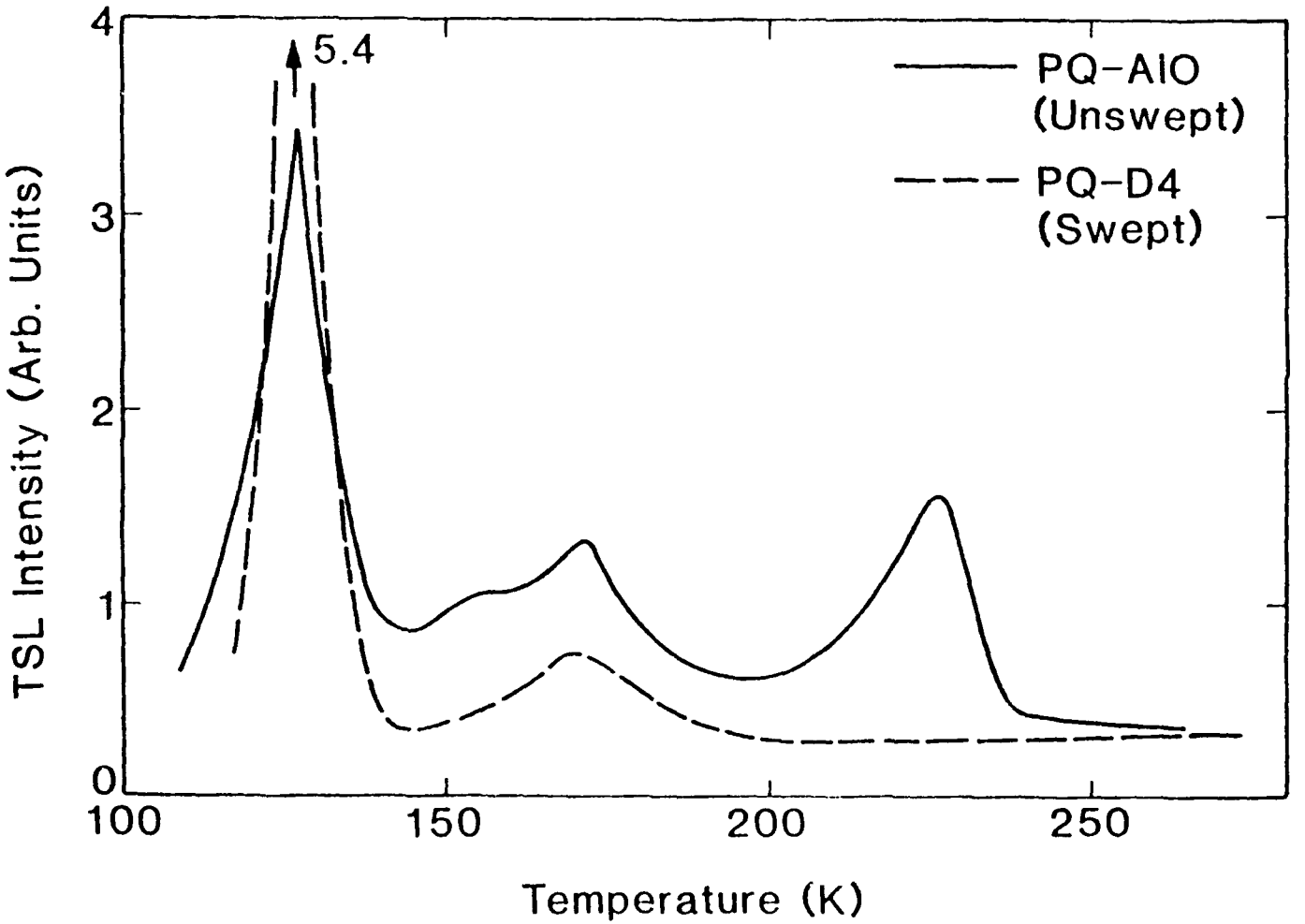

Figure 20. Comparison of TSL intensities vs temperature for unswept (PQ-A10) and swept (PQ-D4) Premium Q specimens. Irradiation temperature was 95 K.

glow peaks in some Electronic Grade samples but were in basic agreement with the results of Region III.

Halliburton et al.[52] have clearly shown that a 300 K irradiation can change the distribution of hydrogen and alkali-metal ions in high-purity quartz. Such a treatment has also been found to change the TSL. After a 300 K irradiation and reirradiation at 95 K, the Region II and III glow peaks are considerably suppressed as can be seen in Fig. 21 while Region I is essentially unaffected. One is reminded that the effect of the 300 K intermediate irradiation can be eliminated by annealing the sample at 750 K for 10 minutes.

In addition, Halliburton et al.[52] have shown that irradiation at temperatures as low as 200 K can enhance the concentrations of Al-OH^- and Al-hole centers while reducing the Al-M^+ center concentration. Corresponding effects were sought in TSL studies. Irradiation of unswept specimens at an intermediate temperature in the 200-300 K range followed by reirradiation at 95 K and a TSL measurement was found to result in a decrease in the height of the Region III glow peak as measured from its initiation point. In Fig. 22 TSL data for two specimens are shown as a function of intermediate irradiation temperature and compared with infrared, ESR, and Q^{-1} data obtained in other local experiments.[28] The comparison with the trend of the Q^{-1} data and the inverse correlation with the infrared and ESR data strongly suggest that all four techniques serve as indicators of the movement of alkali-metal ions away from charge-compensating positions adjacent to aluminum substitutional defects. Some temperature differences are observed but this is not considered surprising in view of the variety of cryostats, mounting and handling techniques, and crystals used. Further evidence that the TSL peak in Region III varies with the Al-M^+ center concentration appears in the first column of Table XII where peak heights measured after single (95 K) and double (300 K and 95 K) irradiations of specimens from several representative bars are included with the other data described.

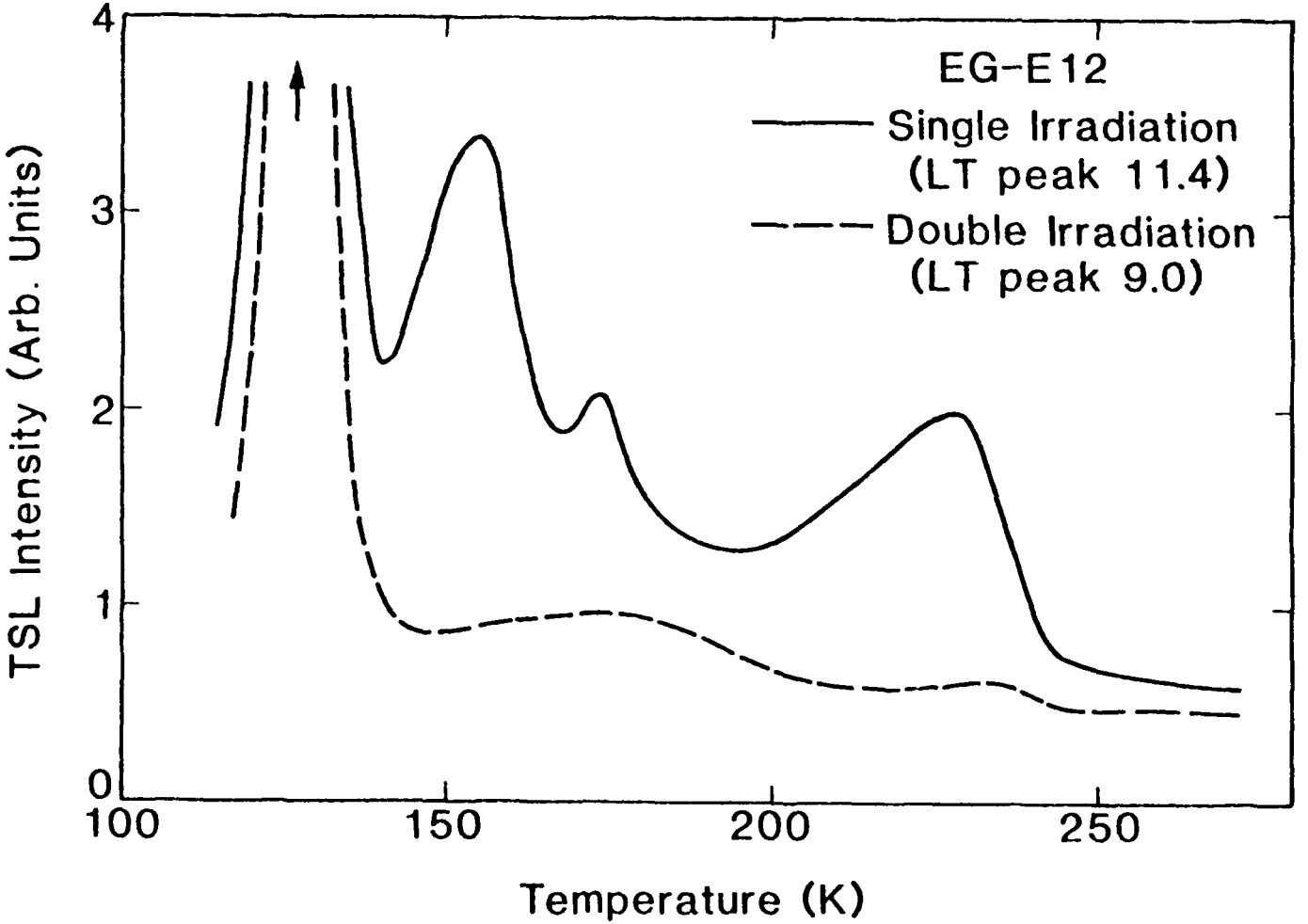

Figure 21. Comparison of TSL intensities vs temperature for an unswept Electronic Grade (EG-E12) specimen following irradiation at 95 K only and irradiation at 15 K preceded by an irradiation at 300 K. Off-scale values of the lowest temperature peak intensities are indicated.

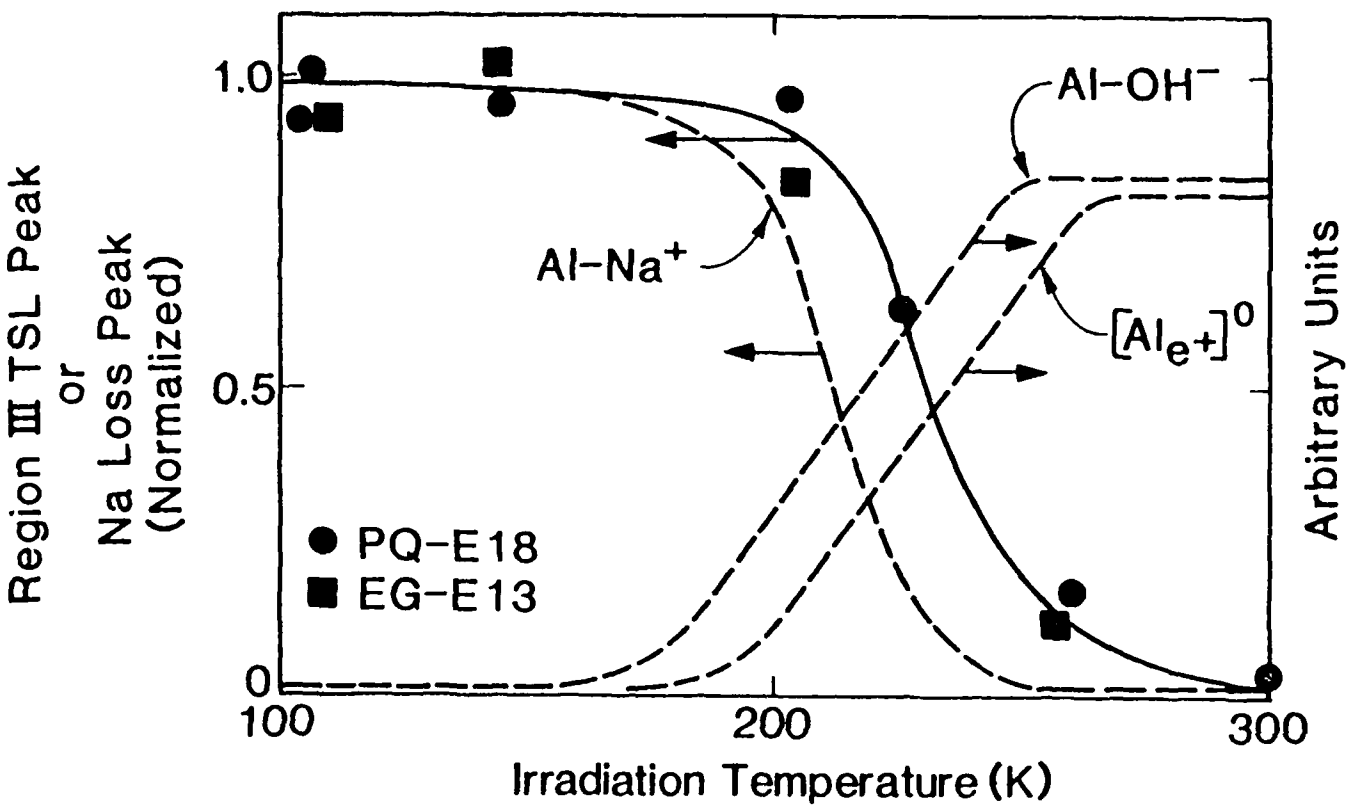

Figure 22. The Region III TSL peak height, AI, decreases when the 95 K irradiation has been preceded by an irradiation above 200 K. The solid curve with data points normalized to the Region III peak height following a single 95 K irradiation illustrates this effect as a function of the prior irradiation temperature for unswept Premium Q (PQ-E18) and Electronic Grade (EG-E13) specimens. Complementary increases in $Al\text{-}OH^-$ and $[Al_{e+}]^0$ centers and decreases in the Na loss peak for similar specimens shown in dashed curves are taken from Reference 22.

Another important effect was observed when samples were irradiated at intermediate temperatures below 300 K and then reirradiated at 90 K for a TSL run. A new, extremely strong glow peak appeared in the 180-210 K region in unswept specimens. Some overlapping of this peak with the regular Region III peak is taken to be responsible for the point scatter in the TSL data of Fig. 22. As shown in Fig. 23, the intensity of the new peak goes through a maximum for an intermediate irradiation temperature of about 200 K. The data plotted are for an unswept Premium Q sample (from bar PQ-E) which was determined by other techniques (see Table XII) to have a particularly high concentration of Al-M^+ centers. Similar, but less pronounced, behavior was observed in an unswept Electronic Grade specimen of lower aluminum content. No such peak appeared in a swept Premium Q sample which also showed no initial Region III peak.

D. Discussion and Conclusions

From previous work[27] there is now good evidence that aluminum impurities and their compensating defects such as H^+ ions in the form OH^- and alkali ions, M^+, are responsible for many important properites of high-purity synthetic quartz. Recent studies at Oklahoma State[52] have emphasized methods for determining the defect concentrations in such crystals using infrared, ESR, and acoustic loss techniques. A related technique, TSL, has been recognized for many years as having the potential to nondestructively measure impurity concentrations and radiation doses. If it can be shown that a TSL glow peak corresponds to the presence of a particular type of defect in quartz and that the intensity of the peak is proportional to the concentration of this type of defect, an important advance will have been made.

The TSL data in Fig. 22 and Table XII strongly suggest that the emission in Region III is due to the presence of Al-M^+ centers and that the intensity of this glow peak is a measure of the concentration of these centers. Thus, it is proposed that the existence and magnitude of the Region III TSL peak in as-grown or annealed

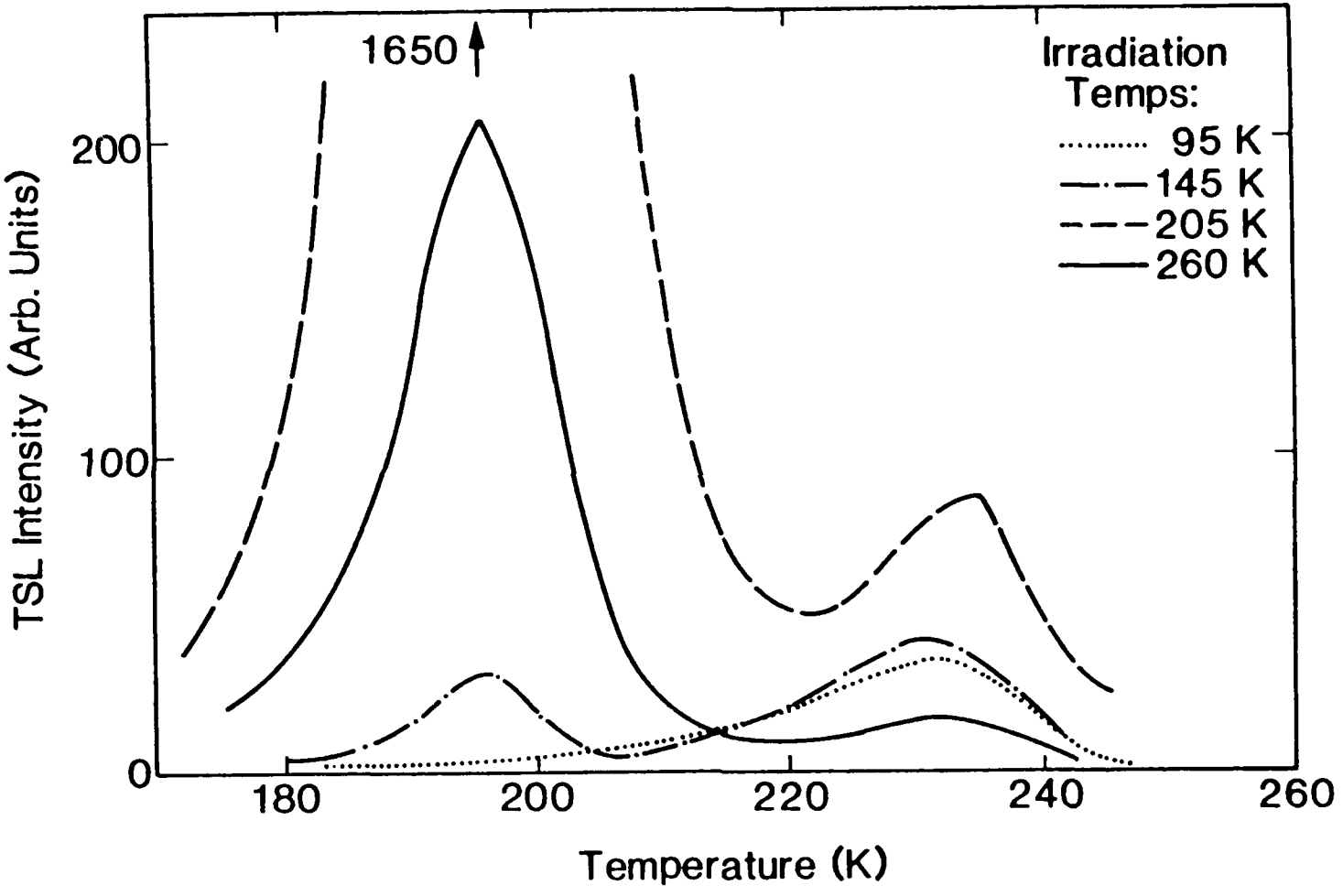

Figure 23. TSL intensity vs temperature for an unswept Premium Q (PQ-E18) specimen as measured following a single 95 K irradiation or a 95 K irradiation preceded by an irradiation carried out at a higher temperature. The limited temperature range of the TSL data presented is chosen to emphasize the appearance of a "new" TSL peak near 200 K.

(750 K) quartz can be used as a nondestructive test for the presence of $Al\text{-}M^+$ defects. This test should improve and simplify the routine evaluation of quartz quality for use in radiation-resistant precision oscillators.

Region I emission occurs in all crystals which have been irradiated at sufficiently low temperature and is tentatively assumed to be due to the presence of hydrogen in the form of hydrogen atoms, H^o. Markes and Halliburton[22] have presented pulsed thermal anneal ESR data which show that H^o centers are present following low temperature irradiation and are thermally destroyed between 115 K and 135 K consistent with the assumption. The recombination process responsible for the 450 nm light is unidentified but release of the hydrogen electron to an Al-hole center is a plausible candidate.

The complexity and variability from sample to sample of the Region II TSL has already been described. The above-referenced[22] pulsed thermal anneal data also indicate the presence and change in number of several unidentified, but probably oxygen-vacancy and/or hydrogen-related, defects in the same temperature region. Recombination processes in this Region -- and in Region III -- must differ from those in Region I as shown by the spectral response results.

Perhaps the most intriguing and unexpected effect found in this investigation was the appearance of the very intense TSL peak in the 180 K-210 K region following a double irradiation procedure in which the first irradiation was carried out at some intermediate temperature between 145 K and 300 K. The origin of this peak is unknown at this time but certainly deserves further study since it may help to elucidate the details of the process by which thermal and irradiation effects combine to dissociate compensating alkali ions from aluminum impurity centers above 200 K. The new peak also shows a correlation with the presence and behavior of the regular Region III peak already proposed as an indicator of $Al\text{-}M^+$ defects, e.g.: 1) maximum magnitudes observed are greater for specimens with higher Region III

peaks, 2) the emission spectrum of the TSL output agrees with that of the Region III peak, and 3) the peak did not appear upon intermediate irradiation of a swept Premium Q specimen which also showed no Region III peak.

Unfortunately, although the effect is large, it is very sensitive to the specific value of the intermediate irradiation temperature (see Fig. 23) and involves multiple operations before a TSL run can be initiated. This leaves the regular Region III peak intensity -- as proposed earlier -- a simpler and more reliable indicator of high-purity crystal quality.

VI. REFERENCES

1. J. C. King and H. H. Sander, IEEE Trans. Nucl. Sci. NS-19, 23 (1972).
2. P. Pellegrini, F. Euler, A. Kahan, T. M. Flanagan, and T. F. Wrobel, IEEE Trans. Nucl. Sci. NS-25, 1267 (1978).
3. T. J. Young, D. R. Koehler, and R. A. Adams, Proceedings of the 32nd Annual Symposium on Frequency Control, 34 (1978). Copies available from the Electronic Industries Association, 2001 Eye Street, N.W., Washington, D.C. 20006.
4. J. C. King, Bell System Technical Journal 38, 573 (1959).
5. R. A. Poll and S. L. Ridgway, IEEE Trans. Nucl. Sci. NS-13, 130 (December, 1966).
6. T. M. Flanagan and T. F. Wrobel, IEEE Trans. Nucl. Sci. NS-16, 130 (December, 1969).
7. B. R. Capone, A. Kahan, R. N. Brown, and J. R. Buckmelter, IEEE Trans. Nucl. Sci. NS-17, 217 (December, 1970).
8. T. M. Flanagan, IEEE Trans. Nucl. Sci. NS-21, 390 (December, 1974).
9. D. B. Fraser, Physical Acoustics, edited by W. P. Mason (Academic, New York, 1968), Vol. 5, Chap. 2.
10. A. Kats, Philips Res. Rep. 17, 133 (1962).
11. R. N. Brown and A. Kahan, J. Phys. Chem. Solids 36, 467 (1975).
12. H. G. Lipson, F. Euler, and A. F. Armington, Proceedings of the 32nd Annual Symposium on Frequency Control, 11 (1978). Copies available from the Electronic Industries Association, 2001 Eye Street, N.W., Washington, D.C. 20006.
13. H. G. Lipson, F. Euler, and P. A. Ligor, Proceedings of the 33rd Annual Symposium on Frequency Control, 122 (1979). Copies available from the Electronic Industries Association, 2001 Eye Street, N.W., Washington, D.C. 20006.

14. W. A. Sibley, J. J. Martin, M. C. Wintersgill, and J. D. Brown, J. Appl. Phys. 50, 5449 (1979).

15. J. H. E. Griffiths, J. Owen, and I. M. Ward, Report of the Bristol Conference - Defects in Crystalline Solids (The Physical Society, London, 1955) p. 81.

16. M. C. M. O'Brien, Proc. Roy. Soc. (London) A231, 404 (1955).

17. J. H. Mackey, Jr., J. Chem. Phys. 39, 74 (1963).

18. J. H. Mackey, J. W. Boss, and D. E. Wood, J. Magn. Res. 3, 44 (1970).

19. R. H. D. Nuttall, Ph.D. dissertation (University of Saskatchewan, 1980) (unpublished).

20. R. Schnadt and J. Schneider, Phys. kondens. Materie 11, 19 (1970).

21. P. R. Barker, J. Phys. C 8, L142 (1975).

22. M. E. Markes and L. E. Halliburton, J. Appl. Phys. 50, 8172 (1979).

23. N. Koumvakalis, J. Appl. Phys. 51, 5528 (1980).

24. J. A. Weil, Radiat. Eff. 26, 261 (1975).

25. Sawyer uses a room temperature infrared test (difference in absorption at 3900 and 3500 cm^{-1}) to distinguish between the two grades of material. The Electronic Grade quartz has a greater hydrogen content.

26. J. E. Wertz and J. R. Bolton, Electron Spin Resonance: Elementary Theory and Practical Applications (McGraw-Hill, New York, 1972) p. 462.

27. L. E. Halliburton, M. Markes, J. J. Martin, S. P. Doherty, N. Koumvakalis, W. A. Sibley, A. F. Armington, and R. N. Brown, IEEE Trans. Nucl. Sci. NS-26, 4851 (1979).

28. S. P. Doherty, J. J. Martin, A. F. Armington, and R. N. Brown, J. Appl. Phys. 51, 4164 (1980).

29. R. A. Weeks and M. Abraham, J. Chem. Phys. 42, 68 (1965).

30. B. D. Perlson and J. A. Weil, J. Magn. Res. 15, 594 (1974).

31. M. E. Markes and L. E. Halliburton (unpublished).

32. L. E. Halliburton, N. Koumvakalis, M. E. Markes, and J. J. Martin, J. Appl. Phys. (in press).

33. D. B. Fraser, J. Appl. Phys. 35, 2913 (1964).

34. J. J. Martin and S. P. Doherty, Proceedings of the 34th Annual Symposium on Frequency Control, U. S. Army Electronics Command, Fort Monmouth, NJ, pp. 81-84 (1980). Copies available from Electronic Industries Association, 2001 Eye Street, N.W., Washington, D.C. 20006.

35. A. W. Warner, Bell System Technical Journal 40, 1193 (1960).

36. J. M. Stevels and J. Volger, Philips Res. Repts. 17, 284 (1962).

37. A. L. Taylor and G. W. Farnell, Can. J. Phys. 42, 595 (1964).

38. R. A. Weeks, J. Appl. Phys. 27, 1376 (1956).

39. R. H. Silsbee, J. Appl. Phys. 32, 1459 (1961).

40. F. J. Feigl, W. B. Fowler, and K. L. Yip, Solid State Commun. 14, 225 (1974); K. L. Yip and W. B. Fowler, Phys. Rev. B 11, 2327 (1975).

41. R. A. Weeks, Phys. Rev. 130, 570 (1963).

42. R. A. Weeks and C. M. Nelson, J. Am. Ceram. Soc. 43, 399 (1960).

43. L. E. Halliburton, B. D. Perlson, R. A. Weeks, J. A. Weil, and M. C. Wintersgill, Solid State Commun. 30, 575 (1979).

44. J. Isoya, J. A. Weil, and L. E. Halliburton, J. Chem. Phys. 74, 5436 (1981).

45. J. H. Anderson and J. A. Weil, J. Chem. Phys. 31, 427 (1959).

46. F. Euler, P. Ligor, A. Kahan, P. Pellegrini, T. M. Flanagan, and T. F. Wrobel, IEEE Trans. on Nuc. Sci. NS-25, 1267 (1978).

47. Sawyer Research Products, Inc., 35400 Lakeland Blvd., Eastlake, Ohio 44094.

48. Toyo Communications Equipment Company, Kawasaki, Japan.

49. R. A. Weeks and M. M. Abraham, Bull. Am. Phys. Soc., Ser. II 10, 374 (1965).

50. R. A. Weeks and M. M. Abraham, excerpt from Solid State Division Annual Progress Report, Oak Ridge National Laboratory, p. 36 (1964).

51. D. L. Griscom, in The Physics of SiO_2 and Its Interfaces, Proceedings of the International Topical Conference, edited by S. T. Pantelides (Pergamon, New York, 1978), pp. 232-252.

52. L. E. Halliburton, N. Koumvakalis, M. E. Markes, and J. J. Martin, to be published J. Appl. Phys. (MS #R-522).

53. R. Yokota, Phys. Rev. 91, 1013 (1958).

54. G. W. Arnold, J. Phys. Chem. Solids 13, 306, (1960).

55. E. N. Batrak, Kristallografiya 3, 104 (1958); 3, 626 (1958) [Sov. Phys. Crystallogr. 3, 102 (1958); 3, 633 (1959)].

56. D. W. McMorris, J. Geophys. Res. 76, 7875 (1971).

57. S. A. Durrani, P. J. Groom, K. A. R. Khazal, and S. W. S. McKeever, J. Phys. D 10, 1351 (1977).

58. W. L. Medlin, J. Chem. Phys. 38, 1132 (1963).

59. M. Schlesinger, J. Phys. Chem. Solids 26, 1761 (1965).

60. P. L. Mattern, K. Lengweiler, and P. W. Levy, Radiat. Eff. 26, 237 (1975).

MISSION
of
Rome Air Development Center

RADC plans and executes research, development, test and selected acquisition programs in support of Command, Control Communications and Intelligence (C^3I) activities. Technical and engineering support within areas of technical competence is provided to ESD Program Offices (POs) and other ESD elements. The principal technical mission areas are communications, electromagnetic guidance and control, surveillance of ground and aerospace objects, intelligence data collection and handling, information system technology, ionospheric propagation, solid state sciences, microwave physics and electronic reliability, maintainability and compatibility.

Printed by
United States Air Force
Hanscom AFB, Mass. 01731

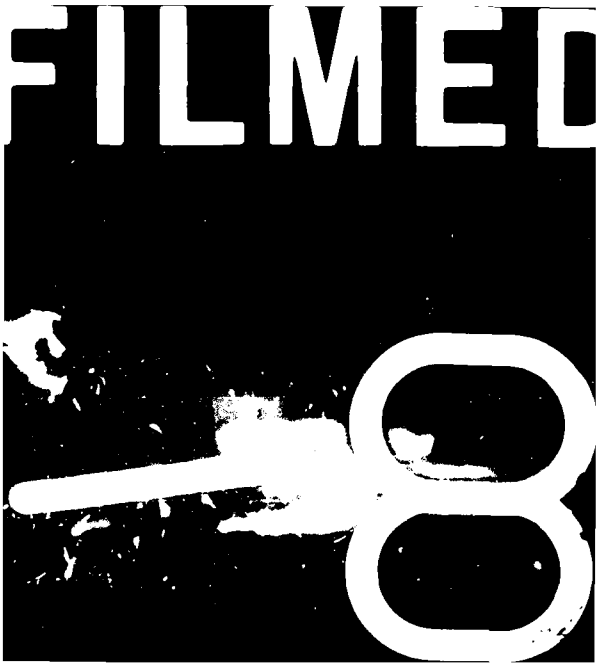
FILMED